VILNIUS UNIVERSITY

FACULTY OF CHEMISTRY AND GEOSCIENCES

INSTITUTE OF CHEMISTRY

LEUNGO KUSHATHA MBAIWA

Nano chemistry and Entrepreneurship

Master thesis

Bacterial Toxin Detection By Using Regenerable Tethered Bilayer Sensors

Scientific adviser

Ausra Valiuniene

Vilnius 2026

CONTENT

LIST OF ABBREVIATIONS

AFM - Atomic force microscopy

αHL - Alpha-hemolysin

ATS - Allyltrichlorosilane

BLM - Black lipid membrane

BV1 - Bacteriorhodopsin variant 1

CPE - Constant phase element

DOPC - 1,2-dioleoyl-sn-glycero-3-phosphocholine

EIS - Electrochemical impedance spectroscopy

FEA - Finite element analysis

FTO - Fluorine-doped tin oxide

HSA - Human serum albumin

ITO - Indium tin oxide

MEM - Membrane

MTS - Methyltrichlorosilane

OTS - Octadecyltrichlorosilane

PBS – Phosphate buffer solution

PDMS - Polydimethylsiloxane

PFT - Pore-forming toxin

SAM - Self-assembled monolayer

SDS - Sodium dodecyl sulfate

SLB - Supported lipid bilayer

SLO - Streptolysin O

stBLM - Sparsely tethered bilayer lipid membrane

tBLM - Tethered bilayer lipid membrane

XPS - X-ray photoelectron spectroscopy

WC14- heptaoxahexatricontane-1-thiol (Wilma compound)

DPhyTL- diphytanyl tetraether lipid

Table of Contents

1. INTRODUCTION

Permeabilising bacterial toxins that induce membrane perforation are no longer merely textbook examples of virulence factors; instead, they represent a significant and ongoing challenge to the safety of food systems, water supplies, and clinical environments.

Toxins such as α-hemolysin produced by *Staphylococcus aureus*, melittin-like peptides, and other pore-forming agents can disrupt membrane integrity even at nanomolar concentrations. Despite their potent biological effects, current detection strategies rely largely on conventional microbiological isolation techniques, costly molecular approaches, and antibody-based assays, which primarily provide indirect evidence of toxin activity by identifying the pathogen's presence [1].

In contrast, lipid membrane-based biosensors offer a promising alternative by enabling direct, biologically relevant detection of toxin-induced membrane disruption. Over the past two decades, substantial progress has been made in designing and developing such biosensing platforms [2].Nevertheless, a critical gap remains between successful laboratory-scale demonstrations and the development of robust, reusable biosensors that function effectively in complex biological matrices, such as blood serum. [3]

Tethered Bilayer Lipid Membranes (tBLMs) have emerged as a promising platform for addressing these challenges in toxin detection. This system combines a biomimetic phospholipid bilayer, a chemically defined submembrane compartment, and a conductive support, enabling the monitoring of membrane integrity using electrochemical impedance spectroscopy (EIS) with gigaohm level sensitivity [4].Ideally, a tBLM-based biosensor would be fabricated on a low-cost, transparent electrode such as fluorine-doped tin oxide (FTO), function effectively in physiologically relevant media, and be fully regenerable. This would allow removal of the lipid bilayer along with bound toxins or serum components after each measurement, while preserving the underlying self-assembled monolayer (SAM) for repeated use with consistent performance [5]. However, this study shows that regeneration remains unreliable under toxin and serum exposure. Instead, a simplified ATS-only SAM architecture on FTO supports stable and reproducible bilayer formation and enables effective toxin detection in a single use format.

Current approaches fall short of these objectives in several respects. First, when regeneration is attempted, the focus is typically on whether the bilayer can be re-formed, rather than on

quantifying the extent of structural damage or evaluating the efficiency of sensor recovery. Second, many tBLM and lipid membrane–based sensors still function effectively as single-use systems, in which the lipid layer is lost during measurement and not systematically regenerated, even though the underlying support remains intact. Recent studies on silane-based tBLMs assembled on fluorine-doped tin oxide (FTO) surfaces have shown that lipid removal and reformation can induce reproducible changes in electrochemical signatures, attributed to alterations in the 1-2 nm submembrane reservoir [6]. Likewise, investigations involving gold-based tBLMs have highlighted the critical role of anchoring chemistry and backfilling molecules in determining toxin sensitivity[6]. However, these studies are largely conducted under controlled buffer conditions, with limited exploration in more complex, physiologically relevant environments such as serum.

The central question addressed in this study can be stated simply: what are the practical limits of regenerating tBLM-based toxin sensors on fluorine-doped tin oxide (FTO), particularly under exposure to pore-forming toxins and blood serum, and which self-assembled monolayer (SAM) architectures provide the most reliable bilayer formation and toxin detection and probably the feasibility of regeneration.

An ideal system would involve a well-defined and stable SAM tBLM assembly on the FTO surface, highly reproducible electrochemical impedance spectroscopy (EIS) responses across repeated measurements, and regeneration processes that preserve the integrity of the submembrane reservoir. Although ambitious, this objective can be divided into two key components that have been widely explored: the development of sensitive and robust sensing platforms, and the design of effective regeneration strategies

Various strategies have been explored to address these challenges. Lipid membrane based biosensors, including planar bilayers, liposomes, and hybrid systems, have demonstrated rapid and sensitive detection of toxins such as aflatoxins and cholera toxin [7].In parallel, benchtop fabricated electrochemical platforms suggest that simple fabrication methods can produce reliable responses to membrane disrupting agents, supporting their potential for real world use [8]. Fundamental studies further highlight the role of lipid composition, bilayer dynamics, and nanoscale architecture in governing pore formation[9]. However, few investigations quantify the impact of repeated regeneration especially in serum-containing environments on submembrane electrical properties or provide frameworks for interpreting impedance shifts under changing baselines.

This limitation has significant consequences. Regeneration-induced changes in submembrane resistance and capacitance can reduce the comparability of toxin response data across cycles, undermining detection reliability [10]. Short-term stability may obscure gradual signal drift, while the need for frequent recalibration weakens the practical benefits of reusable systems [11]. More broadly, the absence of a clear link between regeneration processes, submembrane structure, and sensing performance hinders the rational design of improved tBLM architectures, often resulting in empirically driven development [12].

This study specifically addresses this underexplored area. Building on recent findings that highlight the dominant role of submembrane reservoir properties in regeneration behavior, as well as molecular engineering approaches that tune tBLM sensitivity through SAM composition, we investigate bacterial toxin detection using tBLM sensors fabricated on FTO.

The system is evaluated under both buffer and serum-containing conditions, with regeneration protocols systematically tested across different SAM architectures to determine those that enable reliable bilayer formation and effective toxin sensing.

From a conceptual standpoint, the tBLM/SAM/FTO assembly is treated as a multilayered electrochemical interface, where each component SAM chemistry, submembrane reservoir, lipid bilayer, and adsorbed biomolecules contributes to the overall impedance response [13] .Within this framework, regeneration is viewed not merely as a cleaning process but as a controlled modification of the submembrane environment, the effects of which can be monitored and analysed [14].

The study is guided by the principle that the frequency corresponding to the EIS loss minimum (log f_{min}) reflects a combined influence of defect density and submembrane conductivity [6], [15]. By tracking variations in log f_{min} and related parameters across successive regeneration cycles, it becomes possible to distinguish between toxin-induced effects and changes arising from regeneration.

1.1 Objectives of the study:

1. To fabricate and characterize silane-based and thiol containing selfassembled monolayers (SAMs) on fluorine-doped tin oxide (FTO) including non-conjugated WC14/ATS, conjugated WC14/ATS, WC14-only, and ATS-only systems using contact angle measurements and electrochemical impedance spectroscopy (EIS), in order to evaluate their suitability for supporting high-resistance tBLMs.

2. To assess the EIS response of these membranes to representative pore-forming toxins such as α-hemolysin, as well as the photoresponsive molecule bacteriorhodopsin variant 1 (BV1) under buffered conditions, extracting parameters related to membrane integrity, defect density, and toxin sensitivity.
3. To systematically investigate regeneration protocols involving organic solvents, acids, and detergents across all SAM types following toxin exposure, quantifying regeneration efficiency and identifying conditions that allow reliable bilayer re-formation
4. To determine which SAM architecture offers the most stable and reproducible platform for tBLM-based toxin detection on FTO, even in the absence of complete regeneration, thereby providing design guidelines for low cost, single use or limited use biosensors.

This study holds significance across several dimensions. Academically, it integrates the nanoscale physics of submembrane reservoirs with the analytical chemistry of impedance-based toxin sensing, thereby advancing understanding of the structure and performance of tethered bilayer lipid membranes (tBLMs) in the context of regeneration. From a practical standpoint, distinguishing between regenerated and freshly prepared sensors is crucial for implementing tBLM systems in routine applications, including water, food, and clinical diagnostics. More broadly, this research supports the advancement of sustainable diagnostic technologies, as enhancing biosensor reusability can decrease material consumption and waste while promoting more resource efficient analytical practices.

2. LITERATURE REVIEW

2.1 Tethered Bilayer Lipid Membranes (tBLMs)

Tethered Bilayer Lipid Membranes (tBLMs) are a class of solid-supported model membrane systems in which a phospholipid bilayer is covalently anchored to a conductive or insulating substrate such as gold, fluorine-doped tin oxide (FTO), or silicon oxide via a self-assembled molecular tether layer [16]. In contrast to classical black lipid membranes (BLMs), which are freely suspended and mechanically fragile, or directly supported lipid bilayers (SLBs), which lie in close contact with the substrate and therefore lack sufficient hydration space for protein function, tBLMs incorporate a hydrophilic spacer that forms a defined submembrane aqueous reservoir [13].

This reservoir, typically around 1–2 nm in thickness, separates the lower lipid leaflet from the solid support and plays a critical role in preserving membrane-like behaviour[17]. As a result, tBLMs maintain essential biological properties such as lateral lipid mobility and the capacity to accommodate membrane-associated proteins and pore-forming toxins, while also benefiting from enhanced mechanical stability due to covalent tethering. This stability significantly extends membrane lifetime from only a few hours in BLM systems to weeks or even months in tBLM architectures [18]. By combining biomimetic functionality with structural robustness, tBLMs provide a reliable platform for studying membrane-active processes, particularly the interaction and detection of bacterial pore-forming toxins.

2.1.1 Architectures and Assembly

The properties of tBLMs are strongly influenced by the tethering chemistry and inner leaflet structure. In fully tethered systems, the inner leaflet is composed entirely of anchor lipids bifunctional molecules with a hydrophobic tail, a hydrophilic spacer (often ethylene glycol units), and a surface-binding group such as a thiol or disulfide. Common examples include DPhyTL and WC14, widely used on gold substrates. The outer leaflet is formed by vesicle fusion using lipids such as DOPC or DOPC/cholesterol. These fully tethered architectures provide high electrical sealing, with resistances up to ~55 MΩ·cm² but limit submembrane hydration (~5 vol%) and protein functionality [19].

To overcome this, sparsely tethered bilayer lipid membranes introduce back-filler molecules such as β-mercaptoethanol or ethylene glycol thiols (e.g., C_3EO_5H), which reduce anchor density. This increases submembrane hydration to ~25–60 vol% (10–12), improves lipid

mobility, and enhances functional protein incorporation, making them more suitable for biosensing [20]. The choice of back-filler also affects monolayer organization, with bulkier diluents promoting anchor clustering, lowering membrane viscosity, and increasing toxin sensitivity by up to 7–8-fold compared to simpler back-fillers [7][13].

2.1.1.1 Relevance to Biosensing and Toxin Detection

tBLMs are widely used platforms for investigating membrane-active molecules, with electrochemical impedance spectroscopy (EIS) serving as the primary detection method [14]. When pore-forming toxins or ion channels interact with the membrane, they create conductive pathways that alter the EIS response, typically decreasing membrane resistance and changing interfacial capacitance in a dose-dependent and real-time manner. A well-studied example is α-hemolysin from *Staphylococcus aureus*, which, upon insertion into stBLMs, can reduce membrane resistance by several orders of magnitude [21].

Recent studies have extended this approach toward regenerable sensing systems. (4) demonstrated that tBLMs formed on fluorine-doped tin oxide (FTO) using silane-based anchors can be regenerated after toxin exposure through bilayer removal and reformation. Their work also showed that changes in EIS response across regeneration cycles were primarily linked to alterations in the submembrane reservoir rather than increased membrane defects. These results highlight the importance of controlling submembrane properties to achieve consistent and reliable performance in regenerable tBLM-based toxin sensors, which is the central focus of this study [6].

2.1.1.2 Self-Assembled Monolayers (SAMs)

When certain molecules are introduced to a solid surface in solution, they can spontaneously organize into highly ordered thin films through chemisorption, forming what are known as self-assembled monolayers (SAMs). This process underpins many biosensing and surface engineering applications. In biosensor design, alkanethiol SAMs on gold are widely used, where the thiol group forms a strong Au–S bond with the metal surface, with a bond energy of approximately 170 kJ/mol [22]. On metal oxide substrates such as fluorine-doped tin oxide (FTO), indium tin oxide (ITO), or titanium dioxide, silane-based molecules are more commonly employed. These attach through condensation reactions with surface hydroxyl groups, forming stable covalent Si-O-Si linkage (bond energy 452-465 kJ/mol) [23]. In both systems, lateral van der Waals interactions between alkyl chains promote tightly packed, vertically oriented monolayers, exposing the terminal functional groups at the interface [24].

By selecting appropriate end groups such as hydrophobic methyl, hydrophilic hydroxyl or carboxyl, or biologically active functionalities the surface chemistry can be precisely tuned for specific biosensing applications.

2.1.2 Mixed SAMs as the Anchoring Layer for tBLMs

In tethered bilayer lipid membrane (tBLM)-based sensor systems, the self-assembled monolayer (SAM) serves as more than a simple surface coating. Its molecular-level organisation directly determines the formation, sealing, and function of the overlying lipid bilayer [25]. A widely adopted approach involves preparing mixed, or binary, SAMs by co-depositing an anchor molecule, such as the thiolipids DPTL or WC14 on gold or long-chain octadecyl trichlorosilane (OTS) on fluorine-doped tin oxide (FTO), with a shorter diluent or back-filler molecule, such as β-mercaptoethanol, C3EO5H, or methyltrimethoxysilane on oxide surfaces [25]. Adjusting the ratio of these two components enables control over the packing density and lateral arrangement of anchor groups at the surface, which directly influences the structure of the tBLM inner leaflet [25].

Valincius and colleagues demonstrated that two tBLMs prepared from SAMs with identical bulk composition but different nanoscale clustering of anchor molecules exhibited membrane resistances that differed by three orders of magnitude [21]. This finding indicates that the fine structure of the SAM, rather than its average composition, ultimately governs bilayer electrical integrity.

For metal oxide electrode systems such as FTO, mixed SAMs composed of long-chain OTS, diluted with shorter methyltrichlorosilane (MTS) or vinyltrichlorosilane (VTS), have proven effective in creating the hydrophobic surface required for bilayer deposition [26]. The OTS to MTS ratio in the preparation solution is the primary parameter for tuning surface hydrophobicity [27]. In practice, contact angle measurements are used at this stage to verify that the surface has achieved the appropriate wettability before lipid application.

2.1.3 SAM Stability and Sensor Regeneration

In biosensors designed for repeated use, the self-assembled monolayer (SAM) is critically important, as it must remain physically and chemically stable across multiple cycles of lipid deposition, toxin exposure, and bilayer removal [28]. If the SAM loses its hydrophobic properties or partially desorbs during regeneration, subsequent bilayers may differ from earlier ones, introducing variability that undermines sensor reliability[28].

Research at Vilnius University by Gabriūnaitė and colleagues demonstrated that silane-based SAMs on fluorine-doped tin oxide (FTO) can withstand multiple cycles of bilayer stripping and reformation while maintaining the surface characteristics required to template a new bilayer each time [29]. This finding provides a robust experimental basis for developing regenerable tethered bilayer lipid membrane (tBLM) sensors. Ongoing research focuses on optimising SAM composition, particularly spacer length and back-filler identity, to further enhance the consistency and long-term performance of these regenerable platforms.

2.2 Electrochemical Impedance Spectroscopy (EIS)

Electrochemical impedance spectroscopy (EIS) is a technique used to investigate the electrical behavior of an electrode–solution interface by applying a small sinusoidal alternating potential over a range of frequencies and measuring the resulting current response. Since the applied perturbation is kept minimal, typically around 5-10 mV, the method is essentially non-destructive, making it particularly suitable for sensitive biological systems such as lipid bilayers [30].

The data is shown as a complex impedance spectrum, usually using complex capacitance plots (imaginary versus real impedance) or Bode plots (impedance magnitude and phase versus frequency). These plots show how the interface's resistive and capacitive properties change with frequency.

When the spectra are matched to an equivalent electrical circuit comprising resistors, capacitors, and constant phase elements representing different parts of the system, important values such as membrane resistance and membrane capacitance, can be determined [31]. Each value relates to a specific structural or functional feature of the biosensing interface [32].

Electrochemical impedance spectra were analysed using complex capacitance representation, in which the impedance data $Z(\omega)$ were converted to complex capacitance $C(\omega)$ according to the relationship

$$C^*(\omega) = \frac{1}{j\omega Z^*(\omega)}$$

where j is the imaginary unit, ω is the angular frequency ($\omega = 2\pi f$), and $Z(\omega)$ is the complex impedance [33].

In complex capacitance plots (imaginary capacitance vs. real capacitance), well-formed SAMs and tBLMs exhibit characteristic semicircular features at high frequencies. The capacitance values reported in this work were determined from the diameter of the small high frequency semicircle in the complex capacitance representation. This semicircle corresponds to the membrane or SAM layer properties, with typical values of approximately 10 μF/cm² for SAMs and 0.5-1.5 μF/cm² for intact tBLMs [34].

Larger semicircular features observed at lower frequencies represent defect-related processes and submembrane reservoir contributions, and were not used for membrane capacitance determination [35]. This analysis approach follows established protocols for tBLM characterization [36].

All capacitance values are reported as area-normalized values (μF/cm²) based on the electrode working area of 0.16 cm² and 0.32 cm² .

2.2.1 EIS for Characterising tBLM Formation and Integrity

Electrochemical impedance spectroscopy (EIS) is a step-by-step method used to track how tethered bilayer lipid membrane (tBLM) sensors are put together, starting with the bare electrode, then forming a self-assembled monolayer (SAM), and finally building the full bilayer. Each step changes the impedance spectrum in a clear way. When the SAM forms, it adds a noticeable capacitive effect. Adding the lipid bilayer increases the membrane resistance and lowers the complex capacitance system to values like those found in biological membranes, usually between 0.5 and 1 μF/cm² [13].

Valincius and colleagues developed a detailed framework for interpreting tBLM impedance spectra. They found that the submembrane reservoir affects the response at different frequencies, and this effect is not fully explained by standard circuit models. They also showed that membrane defects produce distinct low-frequency features, which help distinguish between intact and disrupted bilayers [15].

Because of this, EIS can provide detailed information on bilayer formation, packing density, defect density, and defect distribution. This makes EIS especially useful for checking membrane quality before and after regeneration.

2.2.2 EIS Detection of Pore-Forming Toxins

When pore-forming toxins interact with a tethered bilayer lipid membrane (tBLM), they insert into the lipid layer and form channels that allow ions to move between the bulk solution and the region beneath the membrane. This process produces a clear change in the electrochemical impedance spectroscopy (EIS) response, particularly a large drop in membrane resistance, which can decrease by one to three orders of magnitude depending on the amount of toxin present [37]. At the same time, changes in the constant phase element parameters indicate that bilayer packing is disrupted and the membrane's structure is compromised [15]. Studies involving streptolysin O (SLO) on gold-supported lipid membranes have demonstrated that charge-transfer resistance decreases in a concentration-dependent manner, following a first-order exponential decay[37]. This finding establishes a quantitative relationship between toxin dose and impedance response. In addition to single-toxin systems, tethered bilayer lipid membranes (tBLMs) have been used to differentiate pathogenic from non-pathogenic bacteria based on their secreted virulence factors [38]. Bhatt and colleagues showed that electrochemical impedance spectroscopy (EIS) signatures from *Staphylococcus aureus* and *Pseudomonas aeruginosa* were clearly distinguishable from those of non-pathogenic *E. coli*, underscoring the selectivity and diagnostic potential of this sensing approach.

2.2.3 Advantages and Limitations of EIS in Biosensing

Electrochemical impedance spectroscopy (EIS) offers a significant advantage over other electrochemical methods, such as voltammetry or amperometry, because it is label-free and enables real-time detection of binding or membrane-disruption events without chemical modification of the analyte. EIS is highly versatile; a single measurement platform can monitor self-assembled monolayer (SAM) formation, bilayer deposition, toxin exposure, and post-regeneration recovery within a single experimental workflow[39]. This versatility makes EIS particularly suitable for the multi-stage characterization required in regenerable biosensor studies. Nevertheless, a recognised challenge in EIS is the ambiguity that can arise in equivalent circuit modelling. Different circuit configurations may produce equally good fits to the same experimental data, highlighting the importance of selecting models based on physical

reasoning rather than solely on mathematical optimisation[40]. For tethered bilayer lipid membranes (tBLMs), the non-standard impedance response of the submembrane reservoir necessitates modifying or replacing conventional Randles-type circuits with more physically realistic models that account for the geometry of the ionic reservoir and the distribution of defects [15].

2.3 Bacterial Toxins and Their Interaction with Lipid Membranes

Pore-forming toxins (PFTs) represent the largest and most extensively studied class of bacterial virulence factors[41]. These toxins are produced by numerous clinically significant pathogens, such as Staphylococcus aureus, Streptococcus pneumoniae, Escherichia coli, and Clostridium perfringens[41]. The main mechanism of PFTs involves a transition from a soluble monomeric state to a membrane-inserted oligomeric complex that perforates the host cell membrane and forms stable protein channels[41]. These channels facilitate uncontrolled transport of ions, metabolites, and, in some cases, larger molecules[41]. When the membrane loses its integrity, cells experience a range of effects. At low toxin levels, this includes ionic imbalance and osmotic stress. At higher levels, it can lead to cell lysis and necrotic death. Because of these effects, PFTs are key in helping bacteria colonise, damage tissue, and avoid the immune system [41]. Analytically, because they cause clear, concentration-dependent changes in the electrical properties of lipid membranes, they are well-suited for detection with tBLM-based electrochemical biosensors[42].

2.3.1 Alpha-Hemolysin (α-HL)

Alpha-hemolysin (α-HL, or Hla) is one of the most extensively studied pore-forming toxins and serves as the primary model analyte in this thesis[43]. It is a β-barrel PFT secreted by *Staphylococcus aureus*. In solution, α-HL exists as a water-soluble monomer composed of 293 amino acids [44]. Upon encountering a suitable lipid membrane, these monomers bind to the bilayer surface and assemble into a heptameric complex. This undergoes a conformational rearrangement, inserting a 14-stranded β-barrel stem into the membrane to form a transmembrane pore approximately 1.4 nm in diameter [45].

At low concentrations, pores form mainly because of interactions with specific membrane receptors, especially ADAM10 in mammalian cells. At higher concentrations, binding is largely non-specific and occurs via phosphocholine headgroups, so it does not depend on receptors[46]. These pores allow monovalent ions such as sodium and potassium, calcium ions,

ATP, and other small molecules to pass through [47]. Depending on the extent of membrane disruption, this can lead to cell death by apoptosis or necrosis[48].

In tBLM-based biosensing studies, α-hemolysin is widely used as a reference pore-forming toxin due to its well-defined structure and reproducible membrane activity[49]. Its insertion into lipid bilayers produces clear and consistent changes in EIS spectra, most notably a significant decrease in membrane resistance, making it a reliable and quantifiable indicator of toxin activity [50].

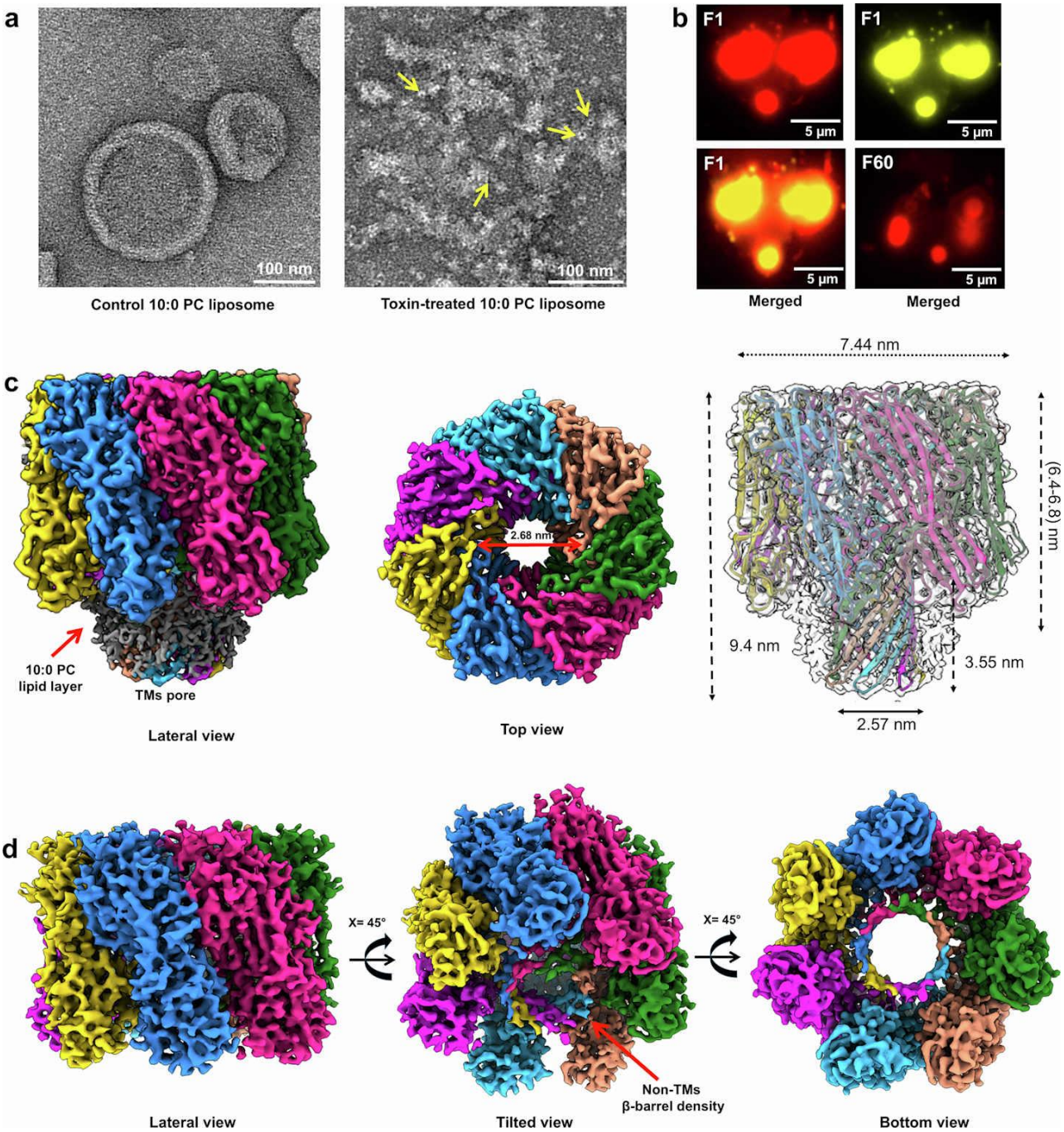

Fig. 1.1 Structural intermediates in α-hemolysin pore formation, showing the transition from pre-pore assembly to the membrane-inserted heptameric β-barrel complex. [51]

2.3.2 Relevance to tBLM-Based Detection

We chose α-hemolysin (α-HL) and melittin as model analytes because their interactions with lipid membranes are well understood, and they have different mechanisms of action. There is also a lot of existing research to help benchmark biosensor performance. α-HL forms β-barrel pores through receptor mediation, while melittin disrupts membranes by directly inserting and partitioning into them[52]. These two approaches offer complementary models for studying membrane disruption. Both toxins produce clear and consistent EIS signatures in tBLM systems, which makes it possible to compare sensor sensitivity and regeneration across different bilayer types and SAM structures[53]. Their importance in medicine also supports their use: α-HL is a major factor in *Staphylococcus aureus* infections like wounds, pneumonia, and sepsis, while melittin is used as a model peptide and has potential as a therapy[54].

These qualities make the sensor system both reliable for analysis and useful for real-world diagnostics.

2.3.3 BV-1

BV-1 is a metal-free, donor–acceptor thiophene-based conjugated molecule engineered to intercalate into biological membranes and respond to visible light [55]. Initially, the literature describes BV-1 as a membrane-targeted photosensitizer for bacterial photodynamic inactivation [55]. Its amphiphilic structure facilitates stable integration into bacterial

membranes, strong absorption in the visible spectrum, and efficient singlet-oxygen generation, which reduces E. coli viability under illumination while exhibiting minimal toxicity in the absence of light [55]. Subsequent studies expanded its application to neuronal membrane modulation, demonstrating that light activation induces membrane phospholipid oxidation, formation of pore-like defects, decreased membrane resistance, and increased cation permeability [56]. These effects enable light-driven depolarization, action potential firing, and optically controlled patch-clamp access or cell death, depending on the stimulation pattern. Collectively, BV-1 is characterized as a versatile molecular nanomachine suitable for imaging-guided photodynamic antibacterial therapy and light-controlled neurobiological interventions[56].

2.4Blood Serum Proteins and Their Interaction with Lipid Membranes

In real biosensing situations, a tBLM sensor is exposed to complex biological fluids such as blood, serum, or plasma rather than purified toxins. These fluids contain many proteins, lipids, and small molecules at normal body concentrations. For example, human serum has about 60-80 mg/mL of total protein, and human serum albumin (HSA) is the most abundant protein, accounting for about 55% [57]. HSA mainly helps transport fatty acids and other small molecules[58]. HSA and other serum proteins can interact with lipid bilayers in a non-specific way, largely due to their surface properties rather than specific binding [59]. This means many serum proteins can attach to phospholipid membranes to some extent. These interactions can alter the bilayer's fluidity, packing, and permeability, which can affect the EIS response of tBLMs in ways unrelated to toxin activity [60]. As a result, they can cause significant interference with measurement.

There are two main challenges in tBLM-based toxin detection. Serum proteins can stick to the membrane surface and also insert themselves into the bilayer. This makes it hard to tell their effects apart from real toxin-induced pore formation in EIS data unless proper controls are used. Research on supported and tethered lipid bilayers shows that exposing them to normal serum or human serum albumin levels can cause major, and sometimes lasting, changes in membrane properties[16]. These changes include higher capacitance and lower resistance [61].

Serum proteins that become embedded in the bilayer may remain there even after washing and can interfere with regeneration. Standard detergent treatments might not completely remove them from the bilayer [62].

For these reasons, it is essential to test regenerable tBLM biosensors in serum-containing media, not just in ideal buffer conditions, to determine if they work in real-world settings. It is also important to see how serum protein adsorption changes the EIS baseline, affects toxin-induced responses, and whether the SAM-supported tBLM system can still be regenerated after being exposed to complex biological environments. These questions are central to this thesis.

2.5Contact Angle Measurements as a Surface Characterization Tool

The shape of a liquid droplet on a solid surface is determined by the balance between cohesive forces within the liquid and adhesive forces between the liquid and the surface. This relationship is quantified by the contact angle (θ), measured at the intersection of the liquid, solid, and vapor phases. A surface with a water contact angle below 90° is classified as hydrophilic, indicating that it attracts water and allows droplets to spread. In contrast, a contact angle above 90° denotes a hydrophobic surface, where water forms beads and exhibits minimal spreading [63] .Recent research has introduced additional categories: surfaces with contact angles below approximately 20° are termed super hydrophilic, while those with angles above approximately 150° are considered superhydrophobic[64]. The most widely used technique for measuring contact angle is static contact angle goniometry[65]. In this approach, a small droplet of deionised water, typically around 5 μL, is deposited onto the surface, and the angle is measured using a goniometer. To ensure accuracy, multiple measurements are performed at different locations on the surface and the results are averaged [66].

2.5.1 Contact Angle as a Diagnostic Tool for SAM Formation

During tBLM sensor fabrication, contact angle measurements provide a straightforward, reliable quality-control method to establish successful self-assembled monolayer (SAM) formation before lipid bilayer deposition. Freshly cleaned fluorine-doped tin oxide (FTO) or gold surfaces are highly hydrophilic, exhibiting water contact angles below approximately 20-30°[67]. Following salinizationor thiol-based SAM assembly, hydrophobic terminal groups are exposed at the interface, resulting in a substantial increase in contact angle, normally 90-110° for well-ordered, densely packed monolayers [68]. The precise contact angle value depends on the composition and packing density of the SAM. For example, long-chain silanes such as octadecyl trichlorosilane (OTS) generate contact angles near 110°, whereas mixed OTS/methyl trichlorosilane (MTS) systems produce intermediate values that correspond to the proportion of long-chain tether molecules [69].

This predictable relationship establishes contact angle measurement as a valuable proxy for assessing surface coverage and tether density, both of which are essential for effective tBLM formation and optimal electrical sealing performance[20].

2.6Monitoring Surface Changes Across Fabrication Steps

In addition to verifying the formation of a self-assembled monolayer (SAM), contact angle measurements are routinely used to monitor each stage of tBLM (tethered bilayer lipid membrane) assembly. Each step produces a characteristic change in surface wettability [70]. Following vesicle fusion and bilayer formation over the SAM, the outermost layer of the tBLM consists of hydrophilic phosphocholine headgroups. This composition significantly decreases the contact angle, returning it to values typical of hydrophilic surfaces, confirming successful bilayer deposition. The sequential progression from bare electrode (low angle) to SAM (high angle) to bilayer (low angle) offers a clear visual and quantitative confirmation of each fabrication stage without the need for complex instrumentation [71]. Any deviation from the expected pattern at any stage alerts the experimentalist to potential issues before further processing [72]. In regenerable sensor systems, contact angle measurements conducted after bilayer removal and prior to redeposition provide an additional verification that the underlying SAM remains intact and retains its hydrophobic properties, which is essential for successful bilayer reformation [73].

2.7Limitations and Complementary Techniques

Although contact angle measurement is a practical and widely used technique, it provides only an indirect, surface-averaged assessment of wettability and cannot independently resolve molecular-scale details such as self-assembled monolayer (SAM) structure, packing order, or defect density [74]. Surface roughness, chemical heterogeneity, and trace contaminants may each independently influence the measured contact angle, independent of SAM quality [75]. Therefore, contact angle data should be interpreted in conjunction with complementary techniques, including electrochemical impedance spectroscopy (EIS), ellipsometry, X-ray photoelectron spectroscopy (XPS), or atomic force microscopy (AFM), to obtain a comprehensive understanding of the modified surface [76]. In the experimental workflow of this thesis, contact angle measurement serves as a rapid screening method to confirm successful salinisation and to verify SAM stability during regeneration cycles, while EIS provides more detailed electrochemical characterisation of both the SAM and the overlying bilayer.

2.8Regenerable tBLM-Based Toxin Sensors

The practical implementation of biosensor platforms in clinical, environmental, or food safety applications depends not only on sensitivity and selectivity but also on cost-effectiveness and reusability. Single-use biosensors, although analytically straightforward, generate considerable material waste, require frequent recalibration, and become cost-prohibitive when processing large sample volumes over time [77]. Regenerable biosensors, which can be cleaned, reset, and reused for multiple detection cycles without significant loss of analytical performance, are therefore essential for translating laboratory-scale biosensor concepts into practical diagnostic tools [78]. In the case of tethered bilayer lipid membrane (tBLM)-based systems, regeneration poses a distinct challenge: the lipid bilayer, serving as the functional sensing element, must be completely removed after toxin exposure, and a new, high-quality bilayer must be reformed on the same self-assembled monolayer (SAM) without compromising the structural integrity of the underlying anchoring layer [79].

2.8.1 Strategies for tBLM Regeneration

Multiple strategies have been documented for regenerating tethered bilayer lipid membrane (tBLM) biosensors following analyte exposure. These methods include mild detergent washing, solvent rinsing, and electrochemical stripping. Both non-ionic and ionic surfactants, such as Triton X-100, sodium dodecyl sulphate (SDS), and commercial detergents like Alconox, have been shown to effectively solubilize and remove the phospholipid bilayer while preserving the underlying self-assembled monolayer (SAM). This preservation enables subsequent deposition of a new bilayer via vesicle fusion [79]. Early studies by Bhosale and colleagues demonstrated that tethered lipid membrane arrays on PDMS microchips could be regenerated using Triton X-100, achieving a relative standard deviation below 4% across three cycles of detection, removal, and regeneration for cholera toxin detection. This finding provided initial evidence that regenerable tBLM platforms could satisfy the reproducibility requirements of quantitative biosensing [80]. More recently, formic acid and urea solutions have been investigated for regeneration after exposure to persistent analytes such as blood serum proteins, which are not completely removed by mild detergents and necessitate more aggressive chemical treatments [78].

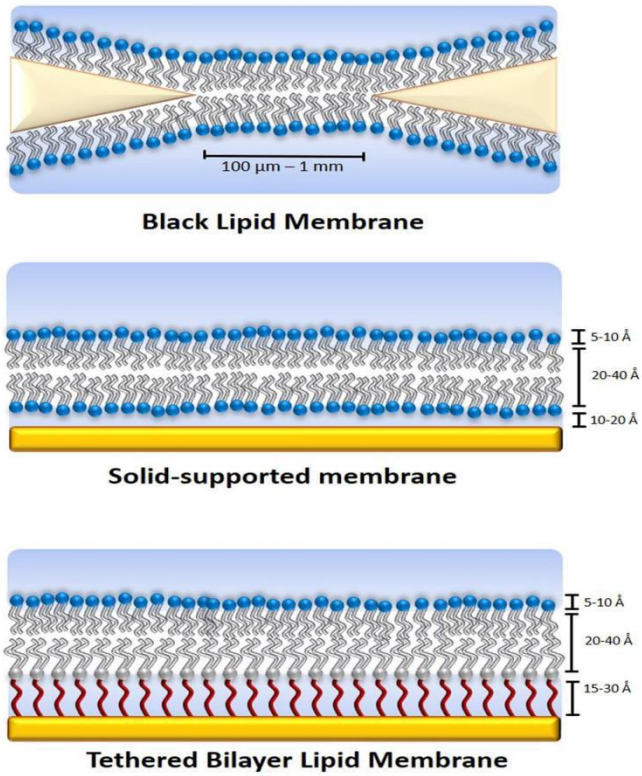

Fig. 2.0 - Comparison of black lipid membrane, solid-supported bilayer and tethered bilayer lipid membrane architectures, illustrating why the tBLM is the preferred platform for regenerable biosensor development. [81]

2.9EIS as a Tool for Monitoring Regeneration Quality

An important advantage of electrochemical impedance spectroscopy (EIS)-based tethered bilayer lipid membrane (tBLM) platforms in regeneration studies is that the same measurement used for toxin detection can also assess bilayer quality after each regeneration cycle, eliminating the need for additional analytical instruments [79]. Following bilayer removal and re-deposition, the EIS spectrum of the regenerated sensor should ideally match that of the freshly prepared sensor, confirming effective resealing of the new bilayer and preservation of the self-assembled monolayer (SAM) properties. However, several studies have reported that although the bilayer reforms successfully, subtle yet systematic changes in EIS parameters accumulate with each regeneration cycle [79][25]. These changes suggest alterations not in the bilayer itself, but in the physicochemical properties of the nanoscale submembrane reservoir located between the bilayer and the SAM [82], [83].

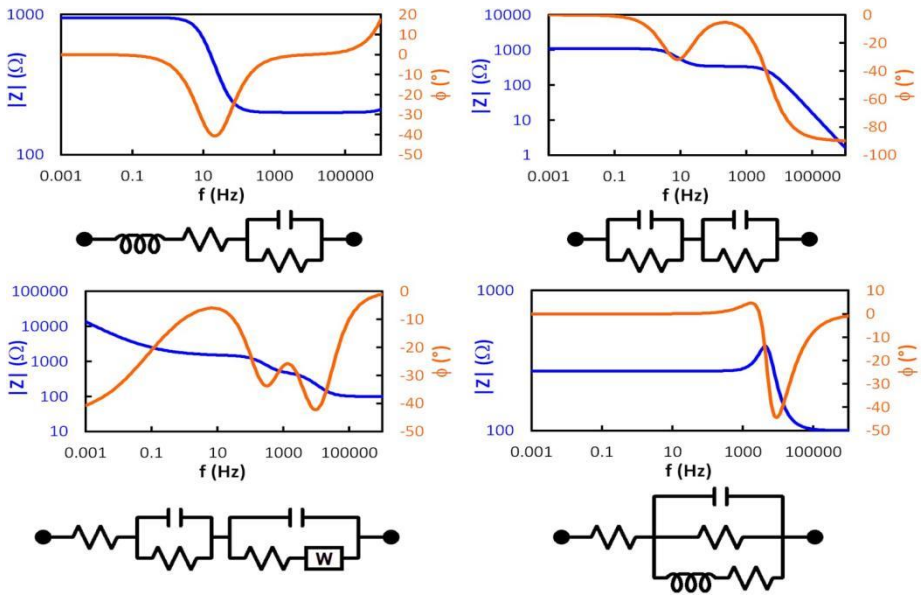

Fig. 2.1- *Representative complex capacitance and Bode plots with equivalent circuit models used to interpret EIS data from tBLM systems before and after regeneration cycles [84]*

2.9.1 Thiol-Based SAMs on Metal and Metal Oxide Surfaces

Thiol-terminated molecules are commonly used as anchors to form self-assembled monolayers on noble metals like gold and silver [85]. The strong bond between metal and sulfur creates stable, tightly packed films that work well for tBLM formation [86].The synthetic thiolipid WC14, which is a PEGylated anchor with a terminal thiol group, is a well-known molecular tether for assembling sparsely tethered bilayer lipid membranes on gold [76]. When used with short thiols such as β-mercaptoethanol, WC14 has been thoroughly studied using electrochemical impedance spectroscopy, neutron reflection, and infrared spectroscopy [76]. In these systems, the metal surface plays a key role: the thiol group attaches directly to the gold, and the resulting self-assembled monolayer forms a clear submembrane reservoir and provides strong electrical sealing for the bilayer above [87].

On metal oxide surfaces such as fluorine-doped tin oxide (FTO), direct chemisorption of thiols is generally regarded as both unfavourable and unstable when compared to silane- or phosphonate-based anchoring chemistries. Comparative studies of molecular anchors on zinc oxide, titanium dioxide, and other oxides have consistently demonstrated that phosphonic acid or silane headgroups produce more robust and reproducible monolayers than thiols [88]. Consequently, most tethered bilayer lipid membrane (tBLM) research on FTO has employed

silane-based self-assembled monolayers (SAMs), such as octadecyl trichlorosilane (OTS) or Methyl trichlorosilane (MTS) , rather than thiol-based anchors [27], [89].

3. Potential Applications of Regenerable tBLM-Based Sensors

Tethered lipid bilayer membranes and related biomimetic membrane platforms have been utilized in a wide range of biotechnological applications, including the investigation of membrane proteins, drug–membrane interactions, and the detection of toxins and pathogens [90]. For instance, tBLM-based "ion-channel switch" biosensors have been employed to detect proteins and viral antigens in complex samples by monitoring changes in ion channel conductance within the tethered bilayer, achieving clinically relevant detection limits and rapid assay times. More broadly, lipid membrane biosensors whether based on tBLMs, supported bilayers, or lipid-coated microstructured electrodes have been developed as rapid, label-free detectors for membrane-disrupting agents such as detergents, antimicrobial peptides, and pore-forming toxins in aqueous samples [91].

These technologies demonstrate significant potential in food safety, where lipid membrane sensors have enabled rapid detection of mycotoxins, bacterial toxins, and pesticide residues in food and water. Such sensors provide portable tools for in-field screening and quality control [92]. In environmental monitoring, lipid-membrane nanosensors have been proposed as early-warning systems for waterborne pollutants that compromise cell membrane integrity [91].In clinical diagnostics, biomembrane-based biosensors are under investigation for the detection of viral particles, bacterial virulence factors, and for high-throughput drug screening targeting membrane-associated proteins. Regenerable tethered bilayer lipid membrane (tBLM) platforms are particularly advantageous for these applications, as they combine the biomimetic recognition capabilities of a lipid bilayer with the capacity for multiple detection cycles on the same sensing surface. This approach reduces per-test costs and material consumption compared to single-use devices [79].

Regenerable tethered bilayer lipid membrane (tBLM) sensors on metal oxide substrates, such as fluorine-doped tin oxide (FTO), show promise, but their use in complex samples such as blood serum remains underexplored [79].The effects of repeated detection and regeneration on submembrane reservoir properties, membrane defects, and toxin sensitivity have not been fully measured [79]. It is also unclear how serum protein adsorption affects regeneration and sensor performance [78].

Filling these knowledge gaps is important for moving tBLM-based toxin sensors from early research to reliable tools for real-world use. This thesis addresses these challenges. While full regeneration was not possible under the tested conditions, finding a simple and affordable ATS

only self-assembled monolayer (SAM) platform that allows for reliable toxin detection is a key step toward practical single-use or limited-use tBLM biosensors.

3.1 Current Gaps and the Contribution of This Thesis

Aleksandrovic et al. (2026) recently made a key advance by studying how tBLMs on FTO substrates can be regenerated. They used silane-based SAMs and DOPC/cholesterol bilayers, exposed the sensors to α-hemolysin, and then regenerated them with a two-step detergent and solvent process. By analysing EIS spectra with inverse modelling, they found that the changes in electrochemical response after each regeneration cycle were not due to more defects in the bilayer. Instead, the main cause was a steady drop in resistance in the 1-2 nm submembrane reservoir, likely because this layer became more hydrated as the SAM was exposed to water during regeneration. This result matters for biosensor design because it shows that regenerated tBLM sensors will produce signals that change in a predictable manner, unlike new sensors [79].

Despite this progress, several questions remain unanswered in the literature. The precise molecular mechanisms driving submembrane hydration during regeneration , including the role of SAM composition, tether density, lipid mixture, and the regeneration agent , have not been systematically studied . Also, the link between submembrane resistance, membrane defect density, and the sensitivity of the toxin detection signal after several regeneration cycles has not been fully established for different toxins or in real samples such as blood serum [79].

These gaps shape the main goals of this thesis: to systematically test whether silane-tethered tBLMS on FTO can be regenerated after exposure to toxins and serum; to measure the success of regeneration across different SAM compositions and washing steps; and to determine which sensor designs, whether regenerable or not, provide the most reliable and repeatable results for toxin detection on FTO [83].

4. MATERIALS

Chemicals and Reagents

- Fluorine-doped tin oxide (FTO) glass slides (18 mm × 25 mm)
- Alconox detergent
- Sulfuric acid (H_2SO_4, 98%)
- Allyltrichlorosilane (ATS)
- WC-14
- Toluene (anhydrous, ≥99.5%)
- 1,2-Dioleoyl-sn-glycero-3-phosphocholine (DOPC)
- Cholesterol (Chol)
- Chloroform (HPLC grade)
- Phosphate-buffered saline (PBS, pH 7.1 and pH 4.4)
- 2-Propanol (isopropanol, ≥99.5%)
- Distilled water (deionized)
- Nitrogen gas (high purity)
- α-Hemolysin (αHL)
- Melittin
- Streptolysin O (SLO)
- Bacteriorhodopsin variant 1 (BV1)
- Fetal bovine serum (FBS)
- Acetone (≥99.5%)
- Acetonitrile (HPLC grade)
- Dimethyl sulfoxide (DMSO, ≥99.9%)
- Formic acid (50% aqueous solution)

Equipment and Instrumentation

- Ultrasonic bath
- Heating plate with temperature control
- Contact angle goniometer (Theta Lite, Biolin Scientific)
- PalmSens potentiostat

- Custom electrochemical cell
- Ag/AgCl reference electrode (saturated NaCl)
- Platinum wire counter electrode
- Micropipettes (1-10 μL, 10-100 μL, 100-1000 μL)
- Lipid extruder
- Polycarbonate extrusion membranes
- Glass Petri dishes
- Glass beakers
- Nitrogen gas supply line
- Analytical balance

5. EXPERIMENTAL METHODS

5.1 Electrode Preparation

Fluorine-doped tin oxide (FTO) glass electrodes (18 mm × 25 mm) served as substrates for self-assembled monolayer (SAM) formation. The cleaning protocol involved initially wiping the FTO surface with a 1% Alconox solution, followed by ultrasonic cleaning in 1% Alconox for 8 minutes. After ultrasonic treatment, the solution was drained, and the electrode was rinsed several times with distilled water. The electrode was subsequently soaked in 98% sulfuric acid for 30 minutes to remove organic residues and activate the surface. After acid treatment, the electrode was thoroughly rinsed with distilled water and subjected to two additional ultrasonic cleaning cycles to remove residual acid. The cleaned electrode was stored in fresh distilled water overnight. SAM formation was conducted the next day.

5.2 Self-Assembled Monolayer (SAM) Formation

Various self-assembled monolayer (SAM) compositions were investigated on FTO electrodes to determine their suitability for supporting tethered bilayer lipid membranes. The SAM preparation procedure was performed using the following method:

Standard SAM formation procedure:

The required mixture of anchor molecules was dissolved in 10 mL of toluene. A cleaned FTO electrode was then immersed in the prepared solution and incubated at 36°C for 1 hour to facilitate self-assembly of the monolayer. Following incubation, the electrode was removed and rinsed successively in four separate beakers containing fresh toluene, with each washing step lasting 3 minutes. During the second washing step, the beaker containing the electrode was maintained at 36°C for 10 minutes and subsequently placed in an ultrasonic bath for 1 minute of sonication while preserving the same temperature. The electrode was then transferred through the third and fourth toluene wash solutions for an additional 3 minutes each. After washing, the electrode was dried using a nitrogen stream and positioned in a Petri dish. Finally, it was heated at 90°C for 1 hour to ensure proper stabilization of the SAM layer.

SAM compositions tested:

1. Non-conjugated WC14 + ATS SAM: 3.94 µL WC-14 + 2.94 µL allyltrichlorosilane (ATS) in 10 mL toluene

2. Conjugated WC14 + ATS SAM: 3.94 µL WC-14 (pre-conjugated) + 2.94 µL ATS in 10 mL toluene.

3. ATS-only SAM: 3.65 µL ATS in 10 mL toluene (no WC-14).

4. WC14-only SAM (control): 3.65 µL WC-14 in 10 mL toluene (no ATS).

All SAM types were prepared following the standard formation protocol described above.

5.3 Contact Angle Measurements

Following SAM formation and heating, the hydrophobicity of the electrode surface was evaluated using static water contact angle measurements. A 5 µL droplet of deionised water was dispensed onto the SAM-coated FTO surface with a micropipette, and the contact angle θ was determined using a contact angle goniometer (Theta Lite, Biolin Scientific). Measurements were conducted at 5 to 8 distinct locations on each electrode to evaluate surface uniformity. A contact angle exceeding 90° was considered indicative of successful hydrophobic SAM formation suitable for bilayer deposition.

Electrochemical Impedance Spectroscopy (EIS) Measurements

Electrochemical impedance spectroscopy (EIS) was employed to characterize the self-assembled monolayer (SAM) and to monitor both membrane formation and toxin-induced alterations. EIS measurements utilized a PalmSens potentiostat with a three-electrode configuration: the SAM or membrane-coated fluorine-doped tin oxide (FTO) electrode as the working electrode, an Ag/AgCl (saturated NaCl) electrode as the reference, and a platinum wire as the counter electrode. Phosphate-buffered saline (PBS, pH 7.1) served as the electrolyte. Impedance spectra were collected over the frequency range 0.1 Hz to 1 MHz at 0 V vs Ag/AgCl with an AC amplitude of 10 mV.

EIS measurements were conducted at several stages: immediately after SAM formation to assess monolayer quality, after bilayer formation to confirm membrane sealing, and after toxin or serum exposure to detect alterations in membrane resistance and capacitance.

5.4 Membrane Formation

When the FTO electrode displayed a sufficiently hydrophobic self-assembled monolayer (SAM), as verified by contact angle measurements, a tethered bilayer lipid membrane was formed using the vesicle fusion method. Lipid vesicles were composed of 1,2-dioleoyl-sn-glycero-3-phosphocholine (DOPC) and cholesterol (Chol) at a 6:4 molar ratio. The lipids (60 µL DOPC and 40 µL Chol) were dissolved in chloroform, dried under nitrogen, and subsequently hydrated in 1 mL phosphate-buffered saline (PBS, pH 4.4) to achieve a final lipid concentration of 1mM. The resulting vesicle suspension was extruded through a polycarbonate membrane to generate small unilamellar vesicles.

The SAM-coated electrode, mounted in a custom electrochemical cell, was initially filled with PBS (pH 7.1) and characterized using electrochemical impedance spectroscopy (EIS). The buffer was then completely removed, and the vesicle suspension was introduced directly into the empty cell. The electrode was incubated for 30 minutes to facilitate vesicle fusion and bilayer formation. Following incubation, excess vesicles were removed by rinsing with fresh PBS (pH 7.1), and EIS measurements were conducted to confirm the formation of a high-resistance membrane.

5.4.1 Toxin and Serum Exposure

Following membrane formation and electrochemical impedance spectroscopy (EIS) characterization, the sensor's capacity to detect pore-forming toxins and respond to biological samples was assessed. The phosphate-buffered saline (PBS) buffer in the electrochemical cell was supplemented with one of the following agents:

Pore-forming toxins, including α-hemolysin (αHL), melittin, streptolysin O (SLO), and bacteriorhodopsin variant 1(BV1), were introduced at varying concentrations to evaluate dose-dependent membrane permeabilization or protein insertion.

Blood serum, either fetal bovine serum (FBS) or human serum, was added at physiologically relevant dilutions to assess sensor selectivity and potential non-specific protein interference.

In certain toxin exposure experiments, sequential additions were performed to observe cumulative or stepwise dose responses. EIS measurements were collected at 30-minute intervals after each addition to monitor changes in membrane resistance and capacitance. For

membranes incorporating BV1, capacitance responses under light exposure were measured using stepwise illumination intervals.

Details regarding toxin type, concentration, and exposure protocol for each experiment are provided in the corresponding Results section alongside the presented data.

5.4.2 Membrane Regeneration

Following exposure to toxin or serum, the sensor underwent regeneration by removing the compromised bilayer while preserving the underlying self-assembled monolayer (SAM) for reuse. The regeneration protocol included the following steps:

1. The cell buffer was removed, and the electrode surface was gently rinsed with phosphate-buffered saline (PBS) to eliminate any residual toxin or serum.

2. The electrode was treated with a washing solution selected from acetone, acetonitrile, dimethyl sulfoxide (DMSO), 50% formic acid, or 1% Alconox detergent solution. Washing was performed at room temperature or at temperatures up to 60°C for 2 to 3 minutes.

3. The electrode was rinsed sequentially with 2-propanol and distilled water, with three rinses performed using each solvent to ensure complete removal of residual washing agents.

4. The electrode was dried under a nitrogen stream and re-characterized by contact angle measurements to assess whether the SAM retained its hydrophobic properties.

5. Electrochemical impedance spectroscopy (EIS) measurements were performed on the washed SAM to confirm complete membrane removal and to verify that impedance values corresponded to those of the bare SAM.

6. If contact angle and EIS measurements indicated that the SAM remained intact and the membrane was successfully removed, fresh lipid vesicles were applied following the procedure described in Section 2.5.

7. After vesicle incubation and rinsing, EIS measurements were performed to verify the re-formation of a high-resistance bilayer. Regeneration was considered successful if the re-formed membrane exhibited impedance characteristics comparable to the initial bilayer (membrane resistance ≥ 1 M$\Omega \cdot cm^2$) and retained sensitivity to subsequent toxin exposures.

6. RESULTS

6.1Non-conjugated WC14 + ATS SAM

Tethered bilayer membrane (tBLM) formation, characterization, and regeneration procedures

Following the methodology outlined in Section 2.2, fluorine-doped tin oxide (FTO) electrodes (area 0.16 cm^2) were functionalized with a self-assembled monolayer (SAM) using a non-conjugated WC14/ATS mixture (3.94 µL WC-14 and 2.94 µL ATS in 10 mL toluene, incubated at 36°C for 1 hour). After the standard washing and heating protocol (90°C, 1 hour), contact angle measurements confirmed successful SAM formation, yielding a hydrophobic surface (θ=103±8°). Electrochemical impedance spectroscopy (EIS) measurements in phosphate-buffered saline (PBS, pH 7.1) were conducted to characterise the SAM. Tethered bilayer membranes were then formed using DOPC:cholesterol (6:4) vesicles prepared in PBS at pH 4.4. After 30 minutes of vesicle fusion, the membrane was characterised by EIS. Subsequently, blood serum was introduced to assess the sensor response, followed by a regeneration attempt using 50% formic acid as the primary washing solvent in figure 3.

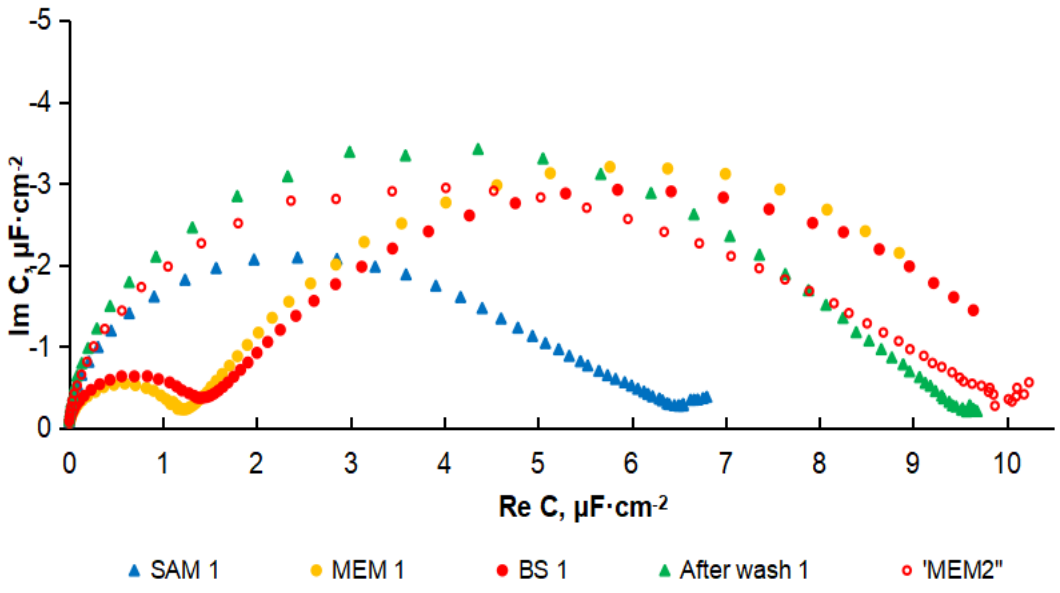

Figure 3: The Complex capacitance representation of the impedance data.

The initial SAM (blue triangles, SAM1) displayed low capacitance values characteristic of a thin monolayer on FTO. The first membrane (yellow circles, MEM1) exhibited decreased capacitance in the range of 1.0µF·cm^{-2}, indicative of successful bilayer formation. After blood

serum exposure (red circles, BS1), the capacitance distribution broadened and shifted, reflecting changes in membrane structure due to protein adsorption. Following treatment with 50% formic acid and rinses with 2-propanol and distilled water, EIS measurements (green triangles, "After wash 1") showed partial recovery toward lower capacitance values, suggesting incomplete bilayer removal. Fresh vesicles were then applied to attempt membrane regeneration, but the regenerated membrane (pink open circles, "MEM2") did not recover the capacitive behavior of the original bilayer, confirming regeneration failure.

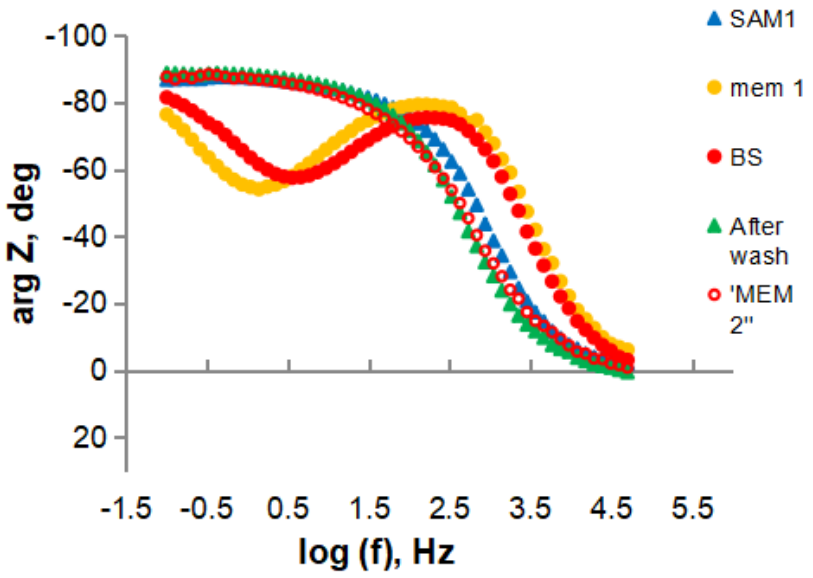

Figure 4: The corresponding EIS spectra in Bode plot format, showing the phase angle as a function of frequency.

The bare SAM (blue triangles, SAM1) exhibited characteristic phase angles around -80° at mid-range frequencies, indicating a capacitive monolayer coating on FTO. Upon vesicle fusion, the membrane (yellow circles, MEM1) showed a shift in the phase response, with phase angles reaching approximately -60° to -70° in the mid-frequency range, consistent with the formation of a bilayer with higher impedance than the bare SAM. Exposure to blood serum (red circles, BS1) resulted in further modification of the phase spectrum. After washing (green triangles, "After wash 1") and attempting regeneration (pink open circles, "MEM2"), the phase spectrum indicated that a stable, high-resistance bilayer had not re-formed.

Comparable washing protocols employing acetone, acetonitrile, and DMSO as primary solvents did not restore functional membrane-forming capacity on WC14/ATS SAMs (data not

shown). These findings suggest that membrane regeneration on non-conjugated WC14/ATS SAMs cannot be achieved through solvent-based washing methods, potentially due to irreversible disruption of the SAM or incomplete lipid removal from the heterogeneous FTO surface.

6.2 Conjugated WC14 + ATS SAM

To determine whether pre-conjugation of the WC-14 component enhances membrane stability and regeneration efficiency, FTO electrodes were functionalized with a conjugated WC-14/ATS self-assembled monolayer (SAM) using identical molar quantities (3.94 µL conjugated WC-14 and 2.94 µL ATS in 10 mL toluene) and the same incubation protocol (36°C for 1 hour) as the non-conjugated system. After SAM formation, a tethered bilayer membrane was assembled using DOPC:cholesterol (6:4) vesicles. The membrane was subsequently exposed to 26 µL of blood serum to assess sensor response. Regeneration was performed by treating the membrane with 1% Alconox detergent solution at 60°C for 3 minutes, followed by rinsing with 2-propanol and distilled water.

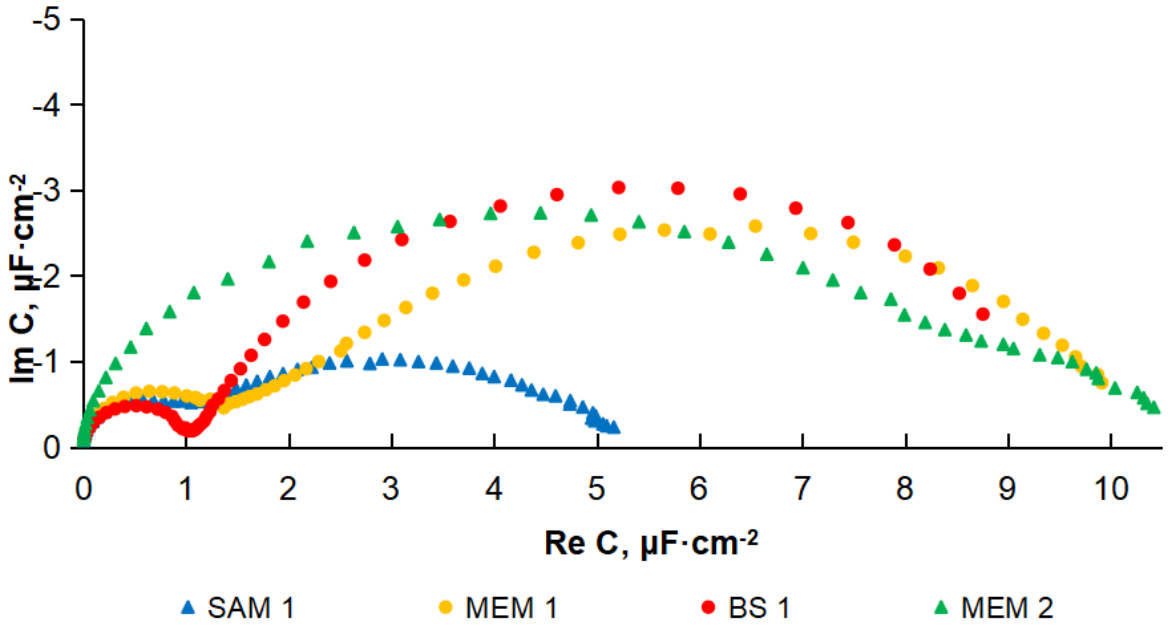

Figure 5: The capacitance plot for the conjugated WC14/ATS system.

The initial self-assembled monolayer (SAM; blue triangles, SAM1) exhibited low capacitance, which is characteristic of a well-formed monolayer. After vesicle fusion, the first membrane (yellow circles, MEM1) demonstrated capacitance of 1.28µF·cm^{-2}, confirming successful

bilayer formation. Subsequent exposure to blood serum (red circles, BS1) resulted in lower capacitance values, , suggesting protein interaction with the membrane. After the Alconox wash at 60°C and the application of fresh vesicles, the attempted regenerated membrane (green triangles, MEM2) exhibited reduced and irregular capacitance behavior, with impedance characteristics shifting toward lower real capacitance values. The trajectory of MEM2 did not recover the smooth semicircular profile observed for the initial membrane, indicating that regeneration was unsuccessful.

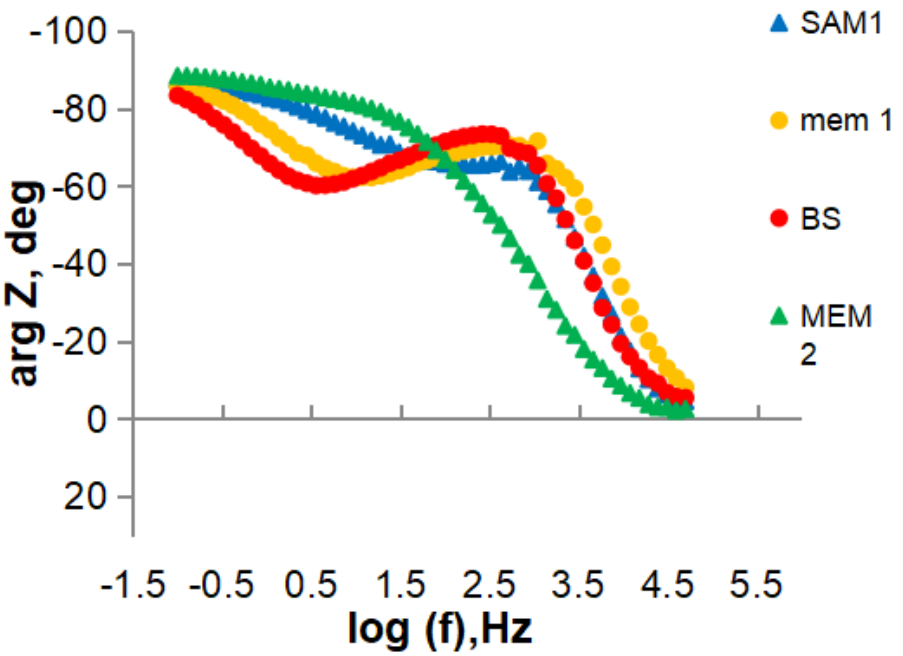

Figure 6: The corresponding Bode plot representation.

The SAM (blue triangles) exhibited phase angles near -80° at mid-range frequencies, consistent with capacitive behavior. The first membrane (yellow circles) showed a phase shift toward -60° to -70°, characteristic of a sealing bilayer. After serum exposure (red circles), the phase response broadened, particularly at lower frequencies. Following washing with Alconox 60% and attempted regeneration (MEM2), the phase spectrum remained distinct from the initial membrane response, with phase angles and frequency characteristics indicating that a stable, high-resistance bilayer had not successfully re-formed.

The results indicate that conjugation of the WC-14 component does not enhance regeneration outcomes relative to the non-conjugated WC14/ATS system. Although heated Alconox detergent may be more effective at lipid removal than organic solvents, it did not restore

membrane-forming capacity. In conjunction with the findings from Section 3.1.1, these results highlight fundamental limitations of WC14/ATS-based self-assembled monolayers for regenerable tethered bilayer lipid membrane sensors on fluorine-doped tin oxide substrates, thereby motivating the exploration of alternative self-assembled monolayer compositions.

6.3 SAM Control Experiments: Comparison of WC14-only, ATS-only, and Mixed SAM Compositions

To determine which self-assembled monolayer (SAM) component facilitated successful membrane formation and to inform the selection of an optimal platform for toxin sensing, control experiments were conducted using single-component SAMs. Fluorine-doped tin oxide (FTO) electrodes were functionalized separately with WC14-only SAM (3.65 µL WC-14 in 10 mL toluene) and ATS-only SAM (3.65 µL ATS in 10 mL toluene), employing the same incubation and heating protocol as used for the mixed systems (36°C for 1 hour, followed by 90°C for 1hour). Electrochemical impedance spectroscopy (EIS) characterization and vesicle fusion experiments were subsequently performed to assess each SAM's capacity to support tethered bilayer formation.

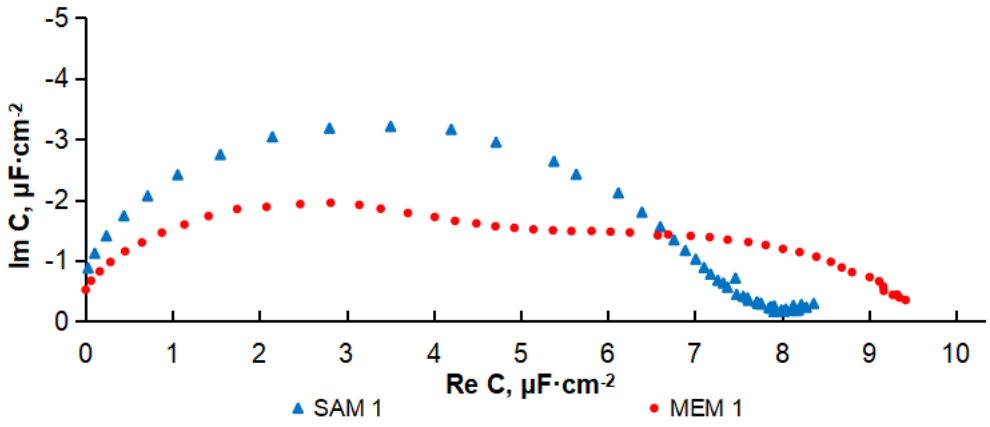

Figure 7: The Capacitance plot for the WC14-only SAM.

The bare (*Figure 7* SAM1) exhibited capacitance values in the range of 6.0 µF·cm^{-2}, significantly higher than typical values for well-ordered monolayers on FTO. This elevated capacitance suggested that the WC14-only layer did not form a dense, insulating coating. When DOPC: cholesterol vesicles were applied following the standard fusion protocol, the

resulting impedance MEM1 showed minimal change from the SAM baseline, with capacitance values remaining around 3.4μF·cm⁻². The complex capacitance plot lacked the characteristic semicircular expansion expected for a sealing bilayer, indicating that vesicle fusion either did not occur or produced only incomplete, defective lipid coverage.

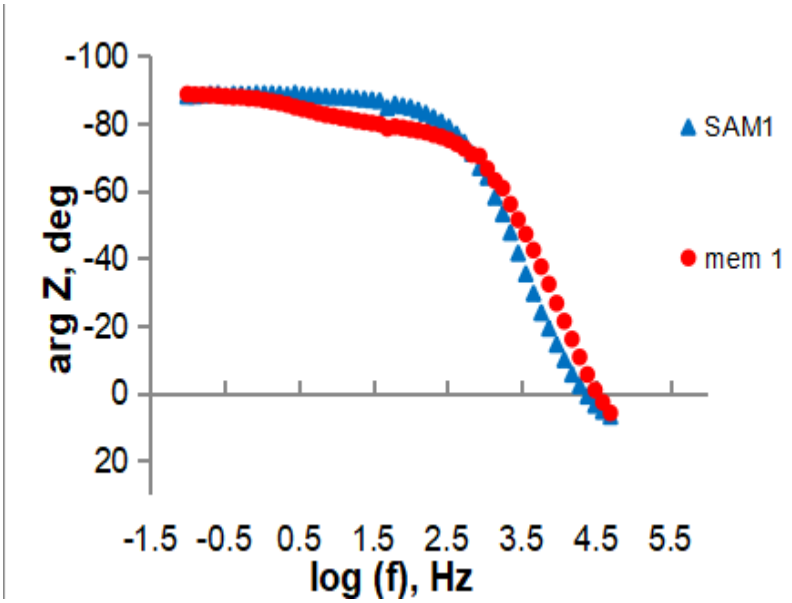

Figure 8: The corresponding Bode plot for the WC14-only SAM.

The WC14-only SAM (*Figure 8,* blue triangles) exhibited phase angles around -80° at mid-range frequencies, but the phase spectrum showed limited frequency-dependent variation. After vesicle addition (red circles), the phase response remained nearly identical to the SAM, with only minor shifts at higher frequencies. The absence of a clear phase transition characteristic of membrane formation confirmed that the WC14-only SAM did not provide a suitable platform for stable tBLM assembly.

6.4 **ATS-only SAM**

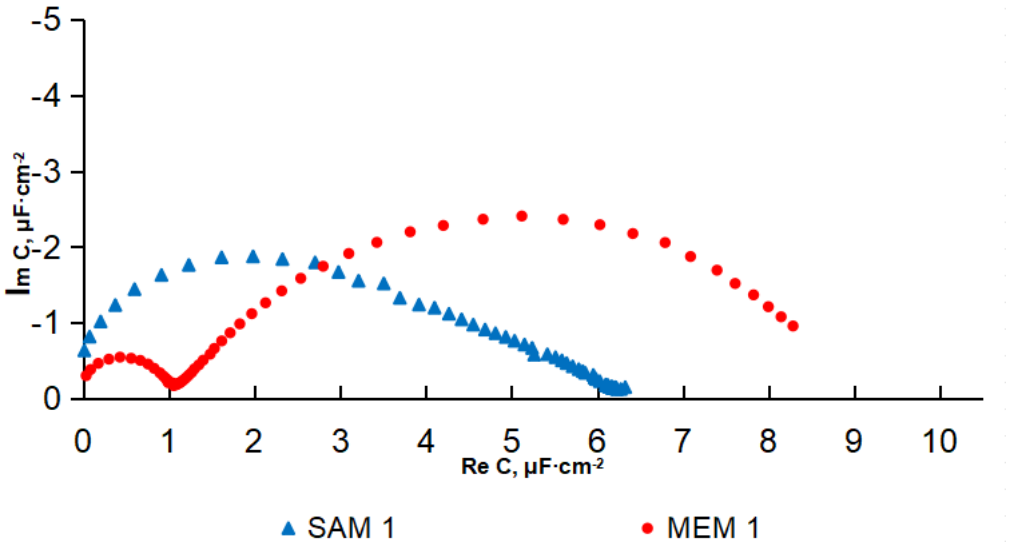

Figure 9 complex capacitance plot for the ATS-only electrode

Compared to the WC14-only system, the ATS-only self-assembled monolayer (SAM) effectively supported robust membrane formation.

Figure 9 presents the complex capacitance plot for the ATS-only electrode. The bare SAM (blue triangles, SAM1) exhibited low capacitance values (3.96 µF·cm^{-2}), which aligns with the presence of a well-ordered, hydrophobic monolayer. After vesicle fusion, the membrane (red circles, MEM1) demonstrated a marked increase in capacitance, reaching -1.0µF·cm^{-2}, and displayed a well-defined semicircular trajectory in the graph. This response is indicative of a high resistance, sealing bilayer that substantially increases the dielectric thickness of the coating.

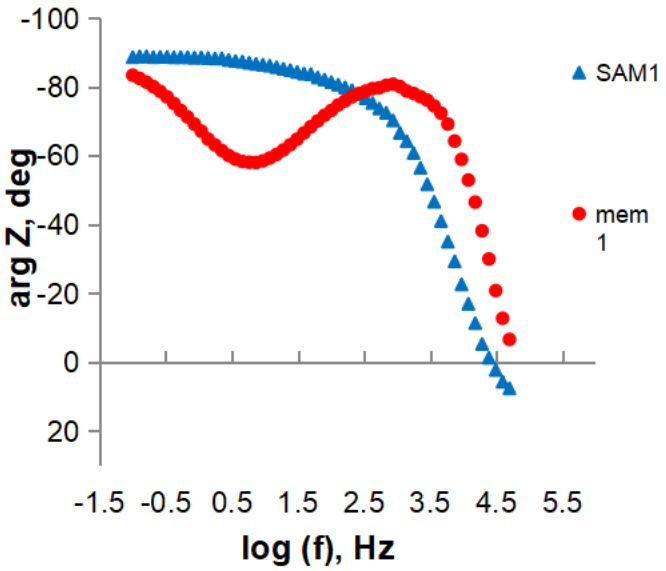

Figure 10: Bode plot for the ATS-only system.

The self-assembled monolayer (*Figure 10,* SAM, blue triangles) exhibited phase angles near -80° across mid-range frequencies, which indicates pronounced capacitive behavior. Following membrane formation (red circles), the phase spectrum shifted toward -60° at characteristic frequencies, consistent with the development of a stable lipid bilayer. The distinct separation between SAM and membrane impedance spectra demonstrates that the ATS-only platform is suitable for tethered bilayer lipid membrane (tBLM) formation.

6.5Comparison and selection of optimal SAM composition

Control experiments demonstrated that ATS-only self-assembled monolayers (SAMs) provided superior performance compared to WC14-only or mixed WC14/ATS systems for tethered bilayer formation on fluorine-doped tin oxide (FTO). The WC14 component did not support vesicle fusion when used alone and, as shown in figure (7) and figure (8), introduced regeneration challenges when combined with ATS. Literature reports indicate that WC14 formulations may contain stabilizing additives and are susceptible to oxidation, both of which could compromise SAM uniformity and membrane stability. Consequently, all subsequent toxin sensing experiments were conducted exclusively on ATS-only SAMs to ensure consistent and high-quality membrane formation.

Table1. Indicating comparison of the capacitance of different SAM compositions

SAM COMPOSITION	Capacitance of SAM ($\mu F \cdot cm^{-2}$) Average ± SD	Capacitance of tBLM ($\mu F \cdot cm^{-2}$) Average ± SD
Non-Conjugated WC14 + ATS	3.94 ± 1.94	01.20± 0.18
Conjugated WC14 + ATS	1.72 ± 0.45	1.12 ± 0.23
WC14 only	6.50 ± 0.14	3.77 ± 0.10
ATS only	4.92 ± 0.82	1.44± 0.58

To make data interpretation easier, samples prepared with different washing methods were grouped by SAM composition. All capacitance values were treated as positive numbers for analysis. The grouped data allowed for clearer comparisons between the different SAM systems while reducing variations from different preparation methods.

6.6 Detection of Bacterial Toxins Using ATS-only Tethered Bilayer Membranes

After the successful formation and characterisation of stable tethered bilayer membranes on ATS-only self-assembled monolayers (SAMs) (Section 3.2.2), the sensor platform was evaluated for its capacity to detect pore-forming bacterial toxins. A-hemolysin (αHL) was chosen as model toxin because of their its established membrane disrupting mechanism and clinical significance.

6.6.1 Dose-dependent αHL detection

To evaluate the sensor's ability to detect concentration-dependent toxin effects, a fresh ATS-only tBLM system was prepared and exposed to sequential additions of αHL at increasing concentrations (50 nM, 75 nM, and 100 nM). EIS measurements were recorded 30 minutes after each toxin addition to monitor the cumulative dose-response behavior.

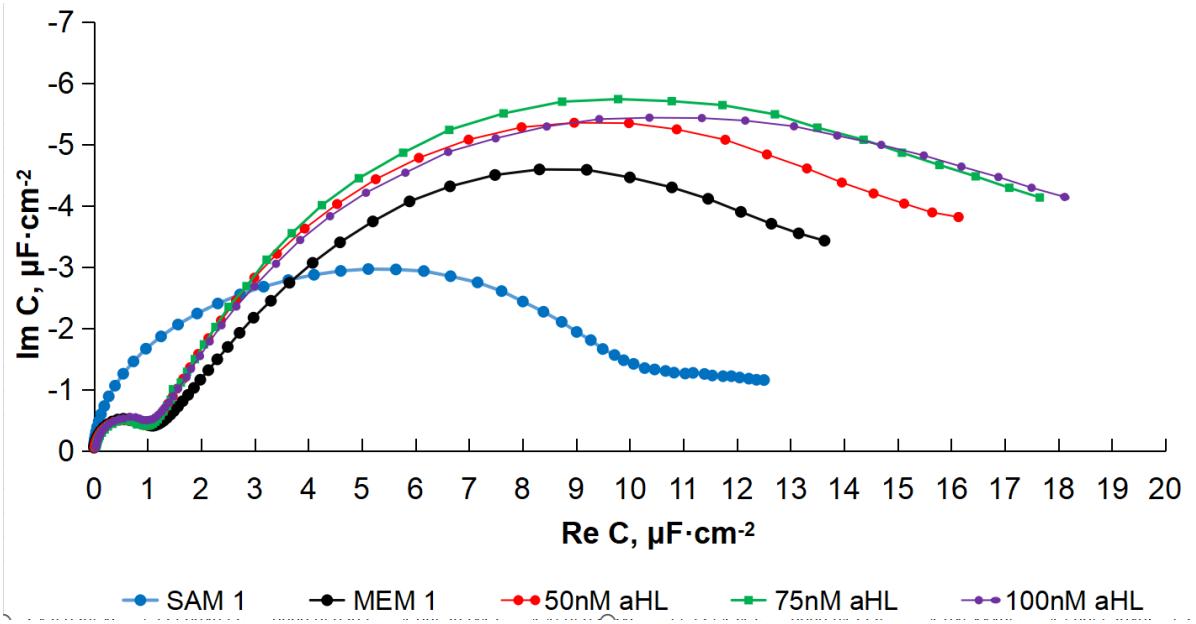

Figure 11: The Complex Capacitance plot for the sequential αHL experiment.

The bare self-assembled monolayer (*Figure 11,* blue circles, SAM1) displayed a capacitance of approximately 10µF·cm⁻². Following membrane formation (black circles, MEM1), the imaginary capacitance decreased to approximately 1.0 µF·cm⁻², accompanied by a well-defined semicircular trajectory, which confirmed the formation of a high-resistance bilayer. Introduction of 50 nM α-hemolysin (αHL; red circles) caused the complex capacitance plot to stay constant at approximately 1.0µF·cm⁻². Subsequent addition to achieve a total αHL concentration of 75 nM (green squares) led to a further decrease in imaginary capacitance to approximately 0.8 µF·cm⁻², while a third addition to 100 nM (purple diamonds) resulted in values approaching 1.0 µF·cm⁻². The consistent upward shift of the semicircles with increasing toxin concentration indicates a clear dose-dependent response, with each αHL addition progressively modifying the membrane's capacitive and resistive properties.

The aHL dose response experiment demonstrated successful toxin detection at 50-100 nM concentrations. The SAM displayed a capacitance of approximately 10 pF-cm-2, which decreased to 1.0 uF-cm-2 following membrane formation. Sequential aHL additions caused progressive upward shifts of the semicircular trajectories, indicating dose-dependent membrane permeabilization. These findings align with published studies by Vockenroth et al. (2008) [12] and McGillivray et al. (2009) [50], which demonstrated functional aHL incorporation into tBLMs on gold substrates. Recent work by Valincius and colleagues showed that optimized mixed SAM architectures achieve 7-8x higher sensitivity than simpler systems, suggesting the ATS-only platform could benefit from further optimization [83]. The 50-100 nM range tested is clinically relevant, as S. aureus secretes aL at concentrations from sub-ug/mL in early infections to ≥10 pg/mL in severe [93].

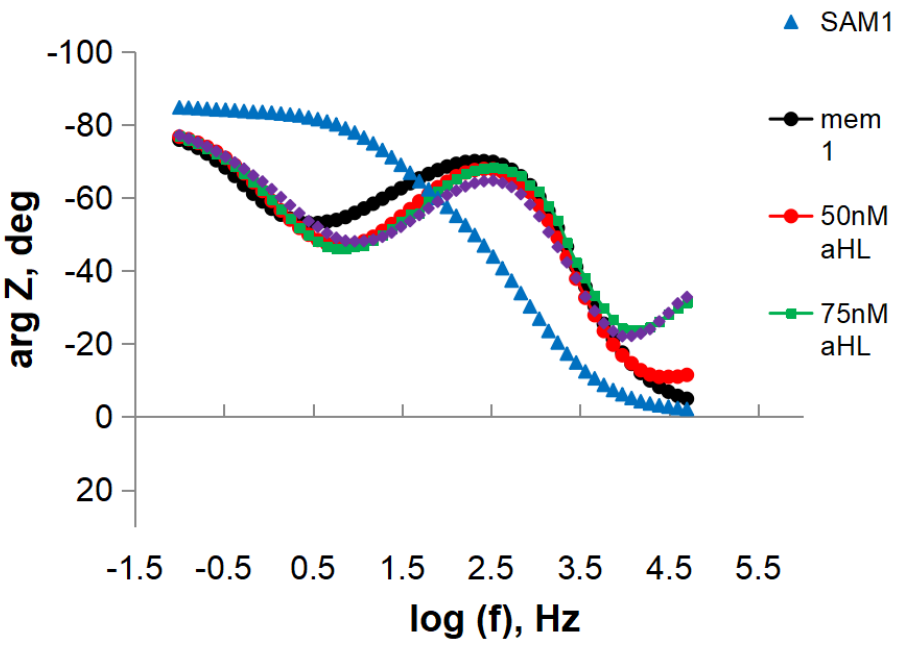

Figure 12: corresponding Bode plot.

The SAM (*Figure 12,* blue circles) showed phase angles near -85° at mid-range frequencies. The membrane (black circles) displayed a typical phase shift toward -65° to -70° around log f = 1-2 Hz. After adding 50 nM αhl (red circles), the phase spectrum stayed similar to the membrane but showed slight changes at specific frequencies. Subsequent additions of αHL to 75 nM (green squares) and 100 nM (purple diamonds) caused gradual shifts in the phase response. These curves overlapped closely at mid-to-high frequencies yet differed at lower frequencies.

The dose-response experiment showed that the ATS-only tBLM platform could detect gradual increases in αHL concentration. The complex capacitance plot offered a clearer distinction between dose levels compared to the Bode plot. The rise in imaginary capacitance with each toxin addition indicated that αHL gradually inserted into and permeabilized the membrane, raising the system's overall capacitance. This dose-dependent response validated the sensor's ability for quantitative toxin detection, although the difference between 50 nM and 100 nM was modest, implying that higher sensitivity or signal boosting methods might be necessary for practical biosensing use.

Sequential aHIL additions caused gradual phase shifts at lower frequencies while mid-to-high frequency responses remained similar-consistent with the defect-based impedance model proposed by Valincius [34], where small toxin pores primarily affect low-frequency submembrane contributions rather than membrane capacitance. This progressive low-frequency shift reflects gradual pore formation rather than catastrophic breakdown.
Although the complex capacitance plot offered clearer dose distinction, the phase data provides complementary mechanistic insight and confirms that the ATS-only FTO platform performs comparably to established gold-based tBLM sensors for qualitative toxin screening [94].

6.7Bacteriorhodopsin variant 1 (BV1) incorporation and photoresponse

To investigate sensing methods beyond pore-forming toxin detection, a final experiment used bacteriorhodopsin variant 1 (BV1). This photo switchable organic molecule spontaneously integrates into lipid membranes and undergoes light-triggered conformational and electronic changes [56]. BV1 was embedded into the DOPC: cholesterol membrane during vesicle formation, and the BV1-containing tBLM was analysed with EIS to assess its photo response. Recent research shows BV1 causes light-induced membrane poration and lipid oxidation, indicating its potential for light-responsive biosensing applications [56].

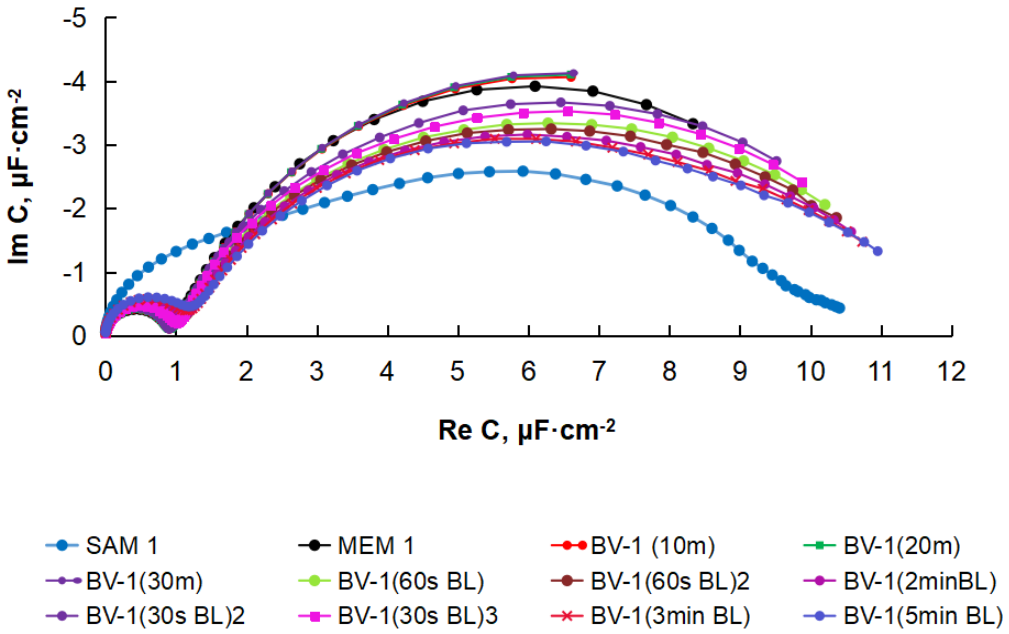

Figure 13 : Complex capacitence for the BV-1 photoresponse .

The bare SAM (*Figure 13,* blue circles, SAM1) 5.14µF·cm^{-2} displayed typical high capacitance values. Following the formation of the BV1-containing membrane (black circles, MEM1), the imaginary capacitance came down to about 0.8 µF·cm^{-2}, signifying successful bilayer assembly. To ensure a stable baseline, EIS measurements were first taken under dark conditions at 10, 20, and 30 minutes after membrane formation (red circles, green squares, and purple diamonds labelled Bv(10m), Bv(20m), Bv(30m), respectively). These dark baseline readings revealed consistent membrane impedance with imaginary capacitance values near 0.8 to 1.2 µF·cm^{-2}, confirming that the BV1-containing membrane remained undamaged over this period without light activation.

Following establishment of the dark baseline, the membrane was exposed to blue light for 30 seconds, after which an EIS measurement was recorded (Bv(30s BL)). Minimal capacitance change was observed after the initial 30-second exposure, prompting subsequent 30-second exposures (Bv(30s BL)2 and Bv(30s BL)3). Due to the limited photoresponse from these short exposures, the light exposure duration was incrementally increased to 60 seconds (yellow-green circles, Bv(60s BL) and Bv(60s BL)2), 2 minutes (brown diamonds, Bv(2min BL)), 3 minutes (orange crosses, Bv(3min BL)), and ultimately 5 minutes (green triangles, Bv(5min BL)).

Complex capacitance plots showed that prolonged cumulative light exposure led to a gradual downward shift in the imaginary part of the capacitance. Following extended light exposures of 2, 3, and 5 minutes, the imaginary capacitance decreased to approximately to 1.0 $\mu F \cdot cm^{-2}$. This observation aligns with the light-induced membrane poration mechanism previously reported for BV1, where illumination initiates charge transfer within the molecule, leading to oxidation of membrane phospholipids and the formation of pore-like structures that enhance membrane conductance and permeability. The observed progressive decrease in capacitance with increasing light exposure duration indicates that cumulative light-driven effects, including lipid oxidation, changes in membrane tension, and pore formation, modified the dielectric and resistive properties of the tBLM.

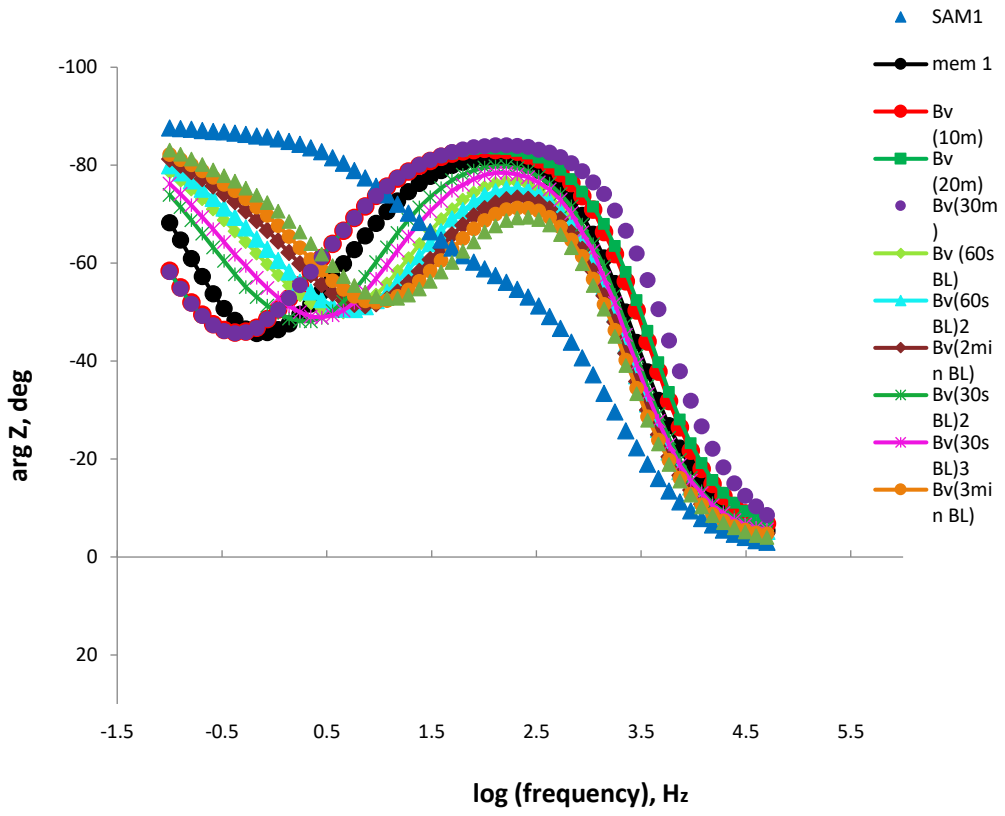

Figure 14 displays the corresponding Bode plot for BV-1 detection.

The SAM (*Figure 14* ,blue circles) exhibited phase angles near -85° at mid-range frequencies, while the BV1-containing membrane (black circles, MEM1) showed a characteristic shift toward -65° to -70°. Dark baseline measurements at 10, 20, and 30 minutes closely overlapped with the initial membrane spectrum. After cumulative light exposure, the phase spectra displayed subtle shifts; however, differentiation between light exposure conditions was less pronounced than in the complex capacitance representation. The Bode plots for various light exposure times remained largely similar, with only minor variations at specific frequencies. These results indicate that capacitance changes observed in the complex capacitance plot serve as more sensitive indicators of BV1 photoresponse than phase angle shifts.

The BV1 experiment demonstrated that the ATS-only tBLM platform can successfully incorporate photoswitchable organic molecules and detect light-induced changes in membrane properties. The dose-dependent photoresponse, in which longer light exposures produced greater capacitance changes, confirms that BV1 remains functionally active within the tethered bilayer and retains its light-responsive characteristics. The observed capacitance decrease is consistent with the reported mechanism of light-triggered pore formation and increased membrane permeability associated with BV1. However, the magnitude of the response was modest, and relatively long cumulative light exposure (multiple minutes) was required to produce clearly measurable impedance changes. These results suggest that the kinetics of BV1 induced membrane modification may be slower in the tBLM configuration compared to free-standing bilayers. This proof of concept result indicates that the FTO-based tBLM platform has potential applications beyond toxin detection, including functional studies of light-activated molecules and the development of optically controlled biosensing systems.

6.8Overview of SAM Performance and Membrane Formation Statistics

A systematic evaluation of the optimal self-assembled monolayer (SAM) formulation for tethered bilayer lipid membrane (tBLM) formation on fluorine-doped tin oxide (FTO) substrates was conducted through comprehensive comparison experiments across all tested SAM compositions. Table 1 presents the membrane formation success rates and regeneration performance for the various silane configurations.

Table 2. Performance comparison of different SAM compositions on FTO substrates

SAM composition on FTO	Cells tested (n)	Initial membranes formed (n)	Initial yield (%)	Cells with regeneration attempt (n)	No of cells with Blood serum (n)	Regenerated membranes (n)	Regeneration yield (%)
Non-conjugated WC-14/ATS (3.94/2.94 µl; main series)	16	16	100%	16	16	0	0%
WC-14 only control (3.65 µl)	2	0	0%	1	0	0	0%
ATS-only control (3.65 µl; single cell)	2	2	100%	0	0	0	0%
Conjugated WC-14/ATS (3.94/2.94 µl)	2	2	100%	2	2	0	0%
ATS-only (3.65 µl)	15	14	93.3%	6	0	1	16.6%

The results indicate that WC-14-only self-assembled monolayers (SAMs) did not support vesicle fusion or membrane formation, with 0% success in two attempts. In contrast, ATS-only SAMs achieved a high membrane formation success rate (93.3%, 14 out of 15 cells), indicating that the shorter-chain silane provided a more suitable hydrophobic surface for lipid bilayer

assembly on fluorine-doped tin oxide (FTO). Mixed WC-14/ATS formulations resulted in 100% initial membrane formation success; however, regeneration attempts were unsuccessful (0% regeneration yield) for all WC-14-containing SAMs. ATS-only SAMs exhibited limited regeneration capability (16.6% yield, 1 out of 6 attempts), which remained inadequate for practical sensor reusability. Therefore, ATS-only SAMs were selected as the optimal platform for all functional experiments due to their high initial formation success, reproducibility, chemical simplicity, and lower cost compared to mixed silane formulations.

7. DISCUSSION

7.1 SAM Selection and Platform Optimization

Initial experiments with WC14 + ATS self-assembled monolayers (SAMs) demonstrated successful membrane formation but revealed significant limitations in regeneration capability and long-term stability. Control experiments comparing WC14-only, ATS-only, and mixed SAM compositions indicated that ATS-only SAMs provided the most effective platform for tethered bilayer formation on fluorine-doped tin oxide (FTO) substrates. The WC14 only SAM did not support vesicle fusion, whereas the ATS-only system consistently produced high-resistance, well-sealed membranes with reproducible impedance characteristics.

7.1.1 Scientific advantages of ATS-only SAMs:

The enhanced performance of ATS results from several molecular and structural factors. Allyltrichlorosilane, a shorter-chain silane, contrasts with WC14, which possesses longer alkyl chains and functional groups designed for bio-conjugation. Shorter alkyl chains in self-assembled monolayers (SAMs) generally produce more compact and densely packed monolayers with fewer defects, thereby offering improved hydrophobic surfaces for lipid membrane anchoring [95]. Previous studies have demonstrated that compact silane monolayers display higher contact angles and reduced surface roughness, both of which are essential for uniform vesicle fusion and effective bilayer sealing.

Furthermore, WC14 formulations often include stabilizing additives and are susceptible to oxidative degradation, which may introduce heterogeneity in SAM quality and reduce long-term stability. In contrast, ATS is a simple and well-defined molecule that forms homogeneous monolayers via strong Si-O-Si covalent bonds to metal oxide surfaces such as fluorine-doped tin oxide (FTO) . The chemical simplicity of ATS minimizes concerns regarding batch-to-batch variability and degradation pathways that are commonly associated with more complex silane reagents.

7.2 Economic advantages of ATS-only SAMs:

The transition to ATS-only self-assembled monolayers (SAMs) provides substantial cost savings compared to gold-based tethered bilayer systems, which remain the standard in many

research laboratories. Gold substrates necessitate costly sputtering or evaporation equipment, vacuum deposition processes, and high-purity gold targets. In contrast, fluorine-doped tin oxide (FTO) glass is commercially available at low cost and is widely utilised in electrochemistry and photovoltaic applications. Self-assembled monolayers (SAMs) with ATS can be formed using microliter-scale quantities of silane reagent via a simple immersion protocol at ~36°C, without requiring specialized equipment. However, the actual amount of ATS required depends on the surface area of the substrate, with larger electrodes requiring proportionally higher volumes.

Additionally, ATS is less costly than WC14 and other functionalized silanes because it lacks bio conjugation groups and complex linker moieties. Removing WC14 from the SAM formulation further reduces reagent expenses without compromising membrane quality. For large-scale or high-throughput biosensing applications, the combination of FTO and ATS offers a cost-effective alternative to traditional gold-thiol or gold-WC14 tethered bilayer lipid membrane (tBLM) platforms, thereby increasing accessibility for resource limited environments and commercial sensor development.

7.3 **Toxin Detection Performance**

The tBLM platform utilizing ATS-only SAMs effectively detected multiple pore-forming toxins, establishing its potential as a label free biosensor for bacterial toxin screening. Detection of α-Hemolysin (αHL) was effective, as clear and reproducible impedance changes were observed with every 30 minutes of exposure to different concentrations. The dose-response experiment (Figure 11) demonstrated systematic increases in capacitance with sequential additions of αHL from 50 nM to 100 nM, confirming the platform's ability to differentiate between varying toxin concentrations.

The response to αHL was more pronounced than that to streptolysin O (SLO) at comparable concentrations. This disparity likely results from differences in the pore-forming kinetics of the two toxins. αHL forms well-characterized heptameric pores that insert rapidly into lipid bilayers, while SLO generates larger, more complex pores that may necessitate extended incubation times or higher concentrations to elicit measurable impedance changes. Previous studies on αHL-membrane interactions report pore formation timescales ranging from seconds to minutes, which aligns with the rapid response observed in the present study.

Detection of toxins at nanomolar concentrations is comparable to that of other tBLM-based sensing platforms reported in the literature, which typically operate within the low-to-mid nanomolar range. Although the observed impedance change was modest, with approximately a 20–30% increase in capacitance at 100 nM αHL, the signal-to-noise ratio enabled reliable detection. The observed dose-dependent response indicates that further optimization may enhance sensitivity.

Gold-based tBLM sensors have been widely investigated for toxin detection and typically demonstrate similar sensitivity ranges (nM to μM) for pore-forming toxins [96]. However, gold platforms involve higher fabrication costs and lack optical transparency, which restricts their application in combined electrochemical and optical sensing approaches. The FTO-based platform developed in this study achieves comparable toxin detection performance and offers additional benefits, including optical transparency, reduced cost, and compatibility with standard electrochemical instrumentation [97].

7.4 **BV1 Incorporation and Functional Protein Studies**

The successful incorporation of bacteriorhodopsin variant 1 (BV1) into the ATS-only tethered bilayer lipid membrane (tBLM) platform, along with the observation of light-induced capacitance changes, marks a significant advancement in the versatility of fluorine-doped tin oxide (FTO)-based membrane sensors. These findings indicate that the platform extends beyond passive toxin detection and is capable of supporting functional investigations of photoactive proteins and molecules.

BV1 is a photoswitchable conjugated organic molecule that integrates into lipid membranes and undergoes light-driven conformational changes, lipid oxidation, and pore formation [98]. The observed progressive decrease in membrane capacitance with increasing light exposure time (Section 6.7) aligns with the established mechanism of BV1-induced membrane poration and enhanced ionic conductance[98]. The dose-dependent photoresponse, in which longer light exposures produced greater capacitance changes, confirms that BV1 maintains its photochemical activity within the tethered bilayer environment.

This proof-of-concept experiment broadens the potential uses of the FTO-based tBLM platform, such as:

Optically-controlled drug delivery systems that utilise light-triggered membrane disruption.

Photodynamic antimicrobial studies that utilise BV1's ability to oxidise lipids.

Light-responsive biosensors, for environmental or clinical diagnostics

Fundamental biophysical studies ,of membrane-protein interactions under optical stimulation

The ability of BV1 to operate within a tethered bilayer on FTO, despite surface heterogeneity and a higher defect density than gold substrates, indicates that the platform is sufficiently robust to host various membrane-active molecules. Future research might investigate other photoactive proteins, such as channelrhodopsin or proteorhodopsin, or photoswitchable lipids to create more advanced light-controlled membrane systems.

7.5 Reasons why regeneration was unsuccessful.

Several factors may contribute to the regeneration challenges observed on FTO substrates:

1. Surface heterogeneity: FTO has a rougher, more varied surface compared to atomically smooth gold or silicon substrates. This roughness can create nanoscale pockets or crevices where lipid material can become trapped, making it difficult to remove by simple washing. Consequently, incomplete lipid removal may prevent the formation of a clean SAM surface needed for subsequent vesicle fusion.

2. SAM Stability: While ATS creates strong Si-O-Si bonds with FTO, the SAM can be partially disturbed by harsh washing conditions like hot detergent or organic solvents. When the SAM is damaged, its hydrophobic nature and uniformity are affected, hindering the formation of high-quality bilayers.

3. Toxin-induced irreversibility: Pore-forming toxins such as αHL embed deeply into the bilayer and might interact with the underlying SAM or substrate. Eliminating the pores along with the lipid membrane could need harsher conditions than those tested here, which might cause irreversible damage to the SAM.

4.Lipid oxidation and cross-linking: Exposure to proteins, serum, or light in the BV1 experiment can cause lipid oxidation and cross-linking, increasing the membrane's resistance to solvent extraction. These oxidised lipids may adhere more strongly to the SAM, requiring enzymatic digestion methods like phospholipase treatment rather than chemical washing.

7.6Comparison to gold-based systems

Literature indicates that regenerating tBLMs on gold substrates remains difficult, with success rates usually under 50% even with optimized methods. The key difference is that gold surfaces can be electrochemically cleaned such as using oxidative potentials to eliminate organic residues without harming the substrate. In contrast, FTO, as a semiconductor instead of a pure metal, might not withstand the same electrochemical cleaning procedures.

Although regeneration was not achieved in this study, the low cost of FTO substrates and the straightforward process of ATS SAM formation suggest that single-use sensors may be economically viable for applications where sensor reusability is not essential. For high-throughput screening or field-deployable diagnostics, disposable FTO-based sensors could provide substantial benefits compared to costly, regenerable gold platforms.

7.7 **Overall Platform Assessment and Outlook**

This study demonstrates that ATS-only self-assembled monolayers (SAMs) on fluorine-doped tin oxide (FTO) substrates provide a functional, cost-effective platform for tethered bilayer lipid membrane formation, toxin detection, and protein incorporation. The principal achievements are as follows:

- Simplified SAM chemistry: The elimination of WC14 reduced both complexity and cost while maintaining membrane quality.
- Nanomolar toxin sensitivity: Detection of αHL was achieved at concentrations of 50–100 nM.
- Functional protein integration: Proof-of-concept photoresponse detection was demonstrated using BV1.
- Economic viability: The FTO and ATS combination is significantly less expensive than gold-thiol systems.

The primary limitation is the lack of regeneration capability, which represents a significant area for future optimization. Nevertheless, due to the platform's affordability, single-use or limited-reuse sensors may be suitable for various applications.

7.8 Future research should concentrate on:

1. Improving regeneration strategies

2. Exploring other short-chain silanes for SAM optimization We believe that there is submembrane reservoir, because aHL was inserted, but more experiments and advanced EIS modelling is needed to understand why rejection of long chain anchor WC14 gives these positive results.

3. Integrating optical detection (leveraging FTO transparency) for multimodal sensing

4. Testing real-world samples (clinical serum, environmental water, food matrices) for toxin detection on FTO-ATS tBLM platform developed in this work represents a significant step toward affordable, accessible membrane-based biosensors for toxin screening, protein studies, and biomedical diagnostics.

Conclusion

The examination effectively demonstrated the viability of an ATS-only self-assembled monolayer (SAM) as a straightforward, affordable substitute, even though a workable mechanism for the post-measurement regeneration of tethered bilayer lipid membranes (tBLMs) was not accomplished during this study. These single-component monolayers demonstrate exceptional stability and repeatability, offering a highly favorable surface design for robust tBLM assembly, as validated by contact angle measurements and subsequent membrane creation. In addition, the ATS-only platform showed performance metrics and structural integrity that were on par with more intricate, multicomponent SAMs. This study successfully confirms the ATS-only SAM as a robust, affordable, and straightforward platform for biosensor development, even if developing efficient regeneration methods is still a crucial goal for future research.

English Summary

This study aimed to develop and characterize a cost-effective, optically transparent tethered bilayer lipid membrane (tBLM) sensor using fluorine-doped tin oxide (FTO) substrates and simplified self-assembled monolayers (SAMs). While traditional gold-based platforms offer high sensitivity for pore-forming toxins, their opacity and high fabrication costs limit their application in combined electrochemical and optical sensing. To address this, an FTO-based platform was developed using an ATS-only anchoring layer. Contact angle measurements and membrane formation assays demonstrated that this single-component ATS monolayer provides a highly stable, reproducible, and economically advantageous architecture, performing comparably to more complex mixed-monolayer systems. The developed FTO/ATS-only platform successfully achieved passive toxin detection with sensitivities comparable to gold based sensors. Furthermore, the versatility of the platform was demonstrated through the successful incorporation of bacteriorhodopsin variant 1 (BV1). Electrochemical investigations revealed a dose-dependent, progressive decrease in membrane capacitance upon light exposure, confirming that BV-1 maintains its photochemical activity and induces membrane poration within the tethered bilayer environment. Finally, the study investigated the potential for sensor reusability through post-measurement membrane regeneration. Although a viable methodology for regenerating the membranes after washing was not achieved, the overall findings validate the ATS-only FTO platform as a robust, low-cost, and transparent foundation. It not only streamlines biosensor fabrication for passive toxin detection but also successfully supports functional investigations of photoactive proteins, establishing a strong baseline for future optimization and regeneration studies.

Summary in Lithuanian

Šio tyrimo tikslas buvo sukurti ir apibūdinti ekonomišką, optiškai skaidrų inkaruotos dvisluoksnės lipidinės membranos (tBLM) jutiklį, naudojant fluoru legiruoto alavo oksido (FTO) padėklus ir supaprastintus savitvarkius monosluoksnius (SAM). Nors tradicinės aukso pagrindu sukurtos platformos pasižymi dideliu jautrumu poras formuojantiems toksinams, jų nepermatomumas ir didelės gamybos išlaidos riboja jų pritaikymą kombinuotuose elektrocheminiuose ir optiniuose tyrimuose. Siekiant išspręsti šią problemą, buvo sukurta FTO pagrindu veikianti platforma, naudojant tik iš ATS junginio sudarytą inkaravimo sluoksnį. Krašto kampo matavimai ir membranų formavimo bandymai parodė, kad šis vieno komponento ATS monosluoksnis sukuria itin stabilią, atkuriamą ir ekonomiškai naudingą architektūrą, kurios savybės prilygsta sudėtingesnėms mišrių monosluoksnių sistemoms.

Sukurta FTO/ATS platforma sėkmingai pritaikyta pasyviam toksinų aptikimui, pasiekiant jautrumą, prilygstantį aukso pagrindo jutikliams. Be to, platformos universalumas buvo įrodytas sėkmingai inkorporuojant bakteriorodopsino 1 variantą (BV1). Elektrocheminiai tyrimai atskleidė nuo apšvietimo trukmės priklausantį laipsnišką membranos talpos mažėjimą, patvirtinantį, kad BV1 išlaiko savo fotocheminį aktyvumą ir indukuoja porų formavimąsi inkaruotoje dvisluoksnėje membranoje.

Galiausiai, tyrime buvo nagrinėjamas jutiklio daugkartinio panaudojimo potencialas, bandant regeneruoti membraną po matavimų. Nors veiksmingos metodikos membranų regeneravimui po plovimo sukurti nepavyko, bendri tyrimo rezultatai patvirtina, kad FTO platforma su ATS monosluoksniu yra tvirtas, pigus ir skaidrus pagrindas. Ji ne tik palengvina biojutiklių gamybą pasyviam toksinų aptikimui, bet ir sėkmingai pritaikoma fotoaktyvių baltymų funkciniams tyrimams, taip sukuriant tvirtą bazę tolimesniems optimizavimo bei regeneracijos tyrimams.

Acknowledgement

I want to thank Jesus Christ for helping me with my education. My sincere thanks go to my supervisor, Prof. Aušra Valiūnienė and Anastasija Aleksandrovič, whom I always went to for consultation. I am grateful for their invaluable guidance, patience, and expertise during this research. Thanks to Prof. Giuseppe Maria Paternò and his research group at Politecnico di Milano for the photosensitizer BV-1. Thanks to the centre for Physical Sciences and Technology (FTMC) for the molecule WC-14. I would like to thank the members of my lab for their support and encouragement, and my family and friends for their constant love and belief in me throughout this journey.

References

[1] S. Guha *et al.*, "Applications and evolution of melittin, the quintessential membrane active peptide," *Biochem. Pharmacol.*, vol. 193, p. 114769, Nov. 2021, doi: 10.1016/j.bcp.2021.114769.

[2] B. J. Berube and J. B. Wardenburg, "Staphylococcus aureus α-Toxin: Nearly a Century of Intrigue," *Toxins*, vol. 5, no. 6, pp. 1140–1166, Jun. 2013, doi: 10.3390/toxins5061140.

[3] G.-P. Nikoleli, C. G. Siontorou, M.-T. Nikolelis, S. Bratakou, and D. K. Bendos, "Recent Lipid Membrane-Based Biosensing Platforms," *Appl. Sci.*, vol. 9, no. 9, p. 1745, Apr. 2019, doi: 10.3390/app9091745.

[4] B. Piro and S. Reisberg, "Recent Advances in Electrochemical Immunosensors," *Sensors*, vol. 17, no. 4, p. 794, Apr. 2017, doi: 10.3390/s17040794.

[5] S. W. Tan, W.-Y. Jeon, B. K. Yoon, and J. A. Jackman, "Mechanistic Evaluation of Antimicrobial Lipid Interactions with Tethered Lipid Bilayers by Electrochemical Impedance Spectroscopy," *Sensors*, vol. 22, no. 10, p. 3712, May 2022, doi: 10.3390/s22103712.

[6] A. Aleksandrovic, I. Gabriunaite, G. Valincius, and A. Valiūnienė, "Regeneration of tethered bilayer lipid membrane biosensors for repetitive use in toxin detection," *Bioelectrochemistry*, vol. 167, p. 109078, Feb. 2026, doi: 10.1016/j.bioelechem.2025.109078.

[7] T. Sabirovas *et al.*, "Molecular engineering of tethered bilayer lipid membranes for impedimetric detection of pore-forming toxins," *Electrochimica Acta*, vol. 508, p. 145226, Dec. 2024, doi: 10.1016/j.electacta.2024.145226.

[8] H. Chen, Y. Zheng, J.-H. Jiang, H.-L. Wu, G.-L. Shen, and R.-Q. Yu, "An ultrasensitive chemiluminescence biosensor for cholera toxin based on ganglioside-functionalized supported lipid membrane and liposome," *Biosens. Bioelectron.*, vol. 24, no. 4, pp. 684–689, Dec. 2008, doi: 10.1016/j.bios.2008.06.031.

[9] S. Saem, O. Shahid, A. Khondker, C. Moran-Hidalgo, M. C. Rheinstädter, and J. Moran-Mirabal, "Benchtop-fabricated lipid-based electrochemical sensing platform for the detection of membrane disrupting agents," *Sci. Rep.*, vol. 10, no. 1, p. 4595, Mar. 2020, doi: 10.1038/s41598-020-61561-7.

[10] A. B. Santa Cruz Garcia, K. P. Schnur, A. B. Malik, and G. C. H. Mo, "Gasdermin D pores are dynamically regulated by local phosphoinositide circuitry," *Nat. Commun.*, vol. 13, no. 1, p. 52, Jan. 2022, doi: 10.1038/s41467-021-27692-9.

[11] I. Gabriunaite *et al.*, "Sensitivity of lipid bilayer sensing of pore-forming toxins relies on electrical properties of nanoscale-thick submembrane reservoir separating solid support and phospholipid membrane," *Electrochimica Acta*, vol. 526, p. 146189, Jun. 2025, doi: 10.1016/j.electacta.2025.146189.

[12] I. K. Vockenroth, P. P. Atanasova, A. T. A. Jenkins, and I. Köper, "Incorporation of α-Hemolysin in Different Tethered Bilayer Lipid Membrane Architectures," *Langmuir*, vol. 24, no. 2, pp. 496–502, Jan. 2008, doi: 10.1021/la7030279.

[13] D. J. McGillivray *et al.*, "Molecular-scale structural and functional characterization of sparsely tethered bilayer lipid membranes," *Biointerphases*, vol. 2, no. 1, pp. 21–33, Mar. 2007, doi: 10.1116/1.2709308.

[14] A. Erbe, R. J. Bushby, S. D. Evans, and L. J. C. Jeuken, "Tethered Bilayer Lipid Membranes Studied by Simultaneous Attenuated Total Reflectance Infrared Spectroscopy and Electrochemical Impedance Spectroscopy," *J. Phys. Chem. B*, vol. 111, no. 13, pp. 3515–3524, Apr. 2007, doi: 10.1021/jp0676181.

[15] G. Valincius, T. Meškauskas, and F. Ivanauskas, “Electrochemical Impedance Spectroscopy of Tethered Bilayer Membranes,” *Langmuir*, vol. 28, no. 1, pp. 977–990, Jan. 2012, doi: 10.1021/la204054g.
[16] S. Shenoy, R. Moldovan, J. Fitzpatrick, D. J. Vanderah, M. Deserno, and M. Lösche, “In-plane homogeneity and lipid dynamics in tethered bilayer lipid membranes (tBLMs),” *Soft Matter*, vol. 2010, no. 6, pp. 1263–1274, 2010, doi: 10.1039/B919988H.
[17] B. Raguse *et al.*, “Tethered Lipid Bilayer Membranes: Formation and Ionic Reservoir Characterization,” *Langmuir*, vol. 14, no. 3, pp. 648–659, Feb. 1998, doi: 10.1021/la9711239.
[18] I. K. Vockenroth, C. Ohm, J. W. F. Robertson, D. J. McGillivray, M. Lösche, and I. Köper, “Stable insulating tethered bilayer lipid membranes,” *Biointerphases*, vol. 3, no. 2, pp. FA68–FA73, May 2008, doi: 10.1116/1.2912097.
[19] S. Tumenas, T. Ragaliauskas, T. Penkauskas, A. Valanciute, F. Ambrulevicius, and G. Valincius, “Solvent effects on composition and structure of thiolipid molecular anchors for tethering phospholipid bilayers,” *Appl. Surf. Sci.*, vol. 509, p. 145268, Apr. 2020, doi: 10.1016/j.apsusc.2020.145268.
[20] D. J. McGillivray *et al.*, “Molecular-scale structural and functional characterization of sparsely tethered bilayer lipid membranes,” *Biointerphases*, vol. 2, no. 1, pp. 21–33, Mar. 2007, doi: 10.1116/1.2709308.
[21] D. J. McGillivray *et al.*, “Structure of Functional Staphylococcus aureus α-Hemolysin Channels in Tethered Bilayer Lipid Membranes”, Accessed: May 17, 2026. [Online]. Available: https://www.cell.com/biophysj/abstract/S0006-3495(08)03231-1
[22] P. Maksymovych, O. Voznyy, D. B. Dougherty, D. C. Sorescu, and J. T. Yates, “Gold adatom as a key structural component in self-assembled monolayers of organosulfur molecules on Au(1 1 1)”, Accessed: May 17, 2026. [Online]. Available: https://impact.ornl.gov/en/publications/gold-adatom-as-a-key-structural-component-in-self-assembled-monol/
[23] C. Haensch, S. Hoeppener, and U. S. Schubert, “Chemical modification of self-assembled silane based monolayers by surface reactions”, doi: 10.1039/B920491A.
[24] “Self-Assembled Monolayers: Advantages of Pure Alkanethiols.” Accessed: May 17, 2026. [Online]. Available: https://www.sigmaaldrich.com/LT/en/technical-documents/technical-article/materials-science-and-engineering/organic-electronics/self-assembled-monolayers
[25] B. Rakovska *et al.*, “Structure and Function of the Membrane Anchoring Self-Assembled Monolayers,” *Langmuir*, vol. 31, no. 2, pp. 846–857, Jan. 2015, doi: 10.1021/la503715b.
[26] M. E. Coda, H. Du, S. Bhandarkar, and D. W. Johnson, “Selected-area sol-gel deposition of barium strontium titanate thin films on thermally oxidized silicon through mediation of self-assembled monolayers,” *Supramol. Sci.*, vol. 4, no. 1, pp. 43–50, Mar. 1997, doi: 10.1016/S0968-5677(96)00056-9.
[27] T. Sabirovas, A. Valiūnienė, I. Gabriunaite, and G. Valincius, “Mixed hybrid bilayer lipid membranes on mechanically polished titanium surface,” *Biochim. Biophys. Acta BBA - Biomembr.*, vol. 1862, no. 6, p. 183232, Jun. 2020, doi: 10.1016/j.bbamem.2020.183232.
[28] O. Seitz *et al.*, “Control and stability of self-assembled monolayers under biosensing conditions”, doi: 10.1039/C1JM10132C.
[29] I. Gabriunaite, A. Valiūnienė, M. Poderyte, and A. Ramanavicius, “Silane-based self-assembled monolayer deposited on fluorine doped tin oxide as model system for pharmaceutical and biomedical analysis,” *J. Pharm. Biomed. Anal.*, vol. 177, p. 112832, Jan. 2020, doi: 10.1016/j.jpba.2019.112832.

[30] C. M. A. Brett, “Electrochemical Impedance Spectroscopy in the Characterisation and Application of Modified Electrodes for Electrochemical Sensors and Biosensors,” *Molecules*, vol. 27, no. 5, p. 1497, Feb. 2022, doi: 10.3390/molecules27051497.
[31] N. Perez and F. Augusto, “Analytical–Computational Integration of Equivalent Circuit Modeling, Hybrid Optimization, and Statistical Validation for Electrochemical Impedance Spectroscopy,” *Electrochem*, vol. 6, no. 4, p. 35, Oct. 2025, doi: 10.3390/electrochem6040035.
[32] E.-M. Korek, R. Teotia, D. Herbig, and R. Brederlow, “Electrochemical Impedance Spectroscopy for Ion Sensors with Interdigitated Electrodes: Capacitance Calculations, Equivalent Circuit Models and Design Optimizations,” *Biosensors*, vol. 14, no. 5, p. 241, May 2024, doi: 10.3390/bios14050241.
[33] G. J. Brug, A. L. G. van den Eeden, M. Sluyters-Rehbach, and J. H. Sluyters, “The analysis of electrode impedances complicated by the presence of a constant phase element,” *J. Electroanal. Chem. Interfacial Electrochem.*, vol. 176, no. 1, pp. 275–295, Sep. 1984, doi: 10.1016/S0022-0728(84)80324-1.
[34] G. Valincius, T. Meškauskas, and F. Ivanauskas, “Electrochemical Impedance Spectroscopy of Tethered Bilayer Membranes,” *Langmuir*, vol. 28, no. 1, pp. 977–990, Jan. 2012, doi: 10.1021/la204054g.
[35] K. J. Kwak *et al.*, “Formation and Finite Element Analysis of Tethered Bilayer Lipid Structures,” *Langmuir*, vol. 26, no. 23, pp. 18199–18208, Dec. 2010, doi: 10.1021/la1021802.
[36] G. Preta, M. Jankunec, F. Heinrich, S. Griffin, I. M. Sheldon, and G. Valincius, “Tethered bilayer membranes as a complementary tool for functional and structural studies: The pyolysin case,” *Biochim. Biophys. Acta BBA - Biomembr.*, vol. 1858, no. 9, pp. 2070–2080, Sep. 2016, doi: 10.1016/j.bbamem.2016.05.016.
[37] T. Wilkop, D. Xu, and Q. Cheng, “Electrochemical Characterization of Pore Formation by Bacterial Protein Toxins on Hybrid Supported Membranes,” *Langmuir*, vol. 24, no. 10, pp. 5615–5621, May 2008, doi: 10.1021/la704027c.
[38] T. N. Tun and A. T. A. Jenkins, “An electrochemical impedance study of the effect of pathogenic bacterial toxins on tethered bilayer lipid membrane,” *Electrochem. Commun.*, vol. 12, no. 10, pp. 1411–1415, Oct. 2010, doi: 10.1016/j.elecom.2010.07.034.
[39] M. Zhang *et al.*, “Electrochemical Impedance Spectroscopy for Real-Time Detection of Lipid Membrane Damage Based on a Porous Self-Assembly Monolayer Support,” *Anal. Chem.*, vol. 90, no. 12, pp. 7422–7427, Jun. 2018, doi: 10.1021/acs.analchem.8b00884.
[40] R. Zhang *et al.*, “Editors’ Choice—AutoEIS: Automated Bayesian Model Selection and Analysis for Electrochemical Impedance Spectroscopy,” *J. Electrochem. Soc.*, vol. 170, no. 8, p. 086502, Aug. 2023, doi: 10.1149/1945-7111/aceab2.
[41] F. R. Ulhuq and G. Mariano, “Bacterial pore-forming toxins,” *Microbiology*, vol. 168, no. 3, p. 001154, 2022, doi: 10.1099/mic.0.001154.
[42] T. Sabirovas, M. Pleckaityte, W. Nogala, V. Shrivastav, and R. Budvytyte, “Imaging functional bacterial pore-forming toxins in tethered bilayer lipid membranes using scanning electrochemical microscopy,” *Bioelectrochemistry*, vol. 165, p. 108953, Oct. 2025, doi: 10.1016/j.bioelechem.2025.108953.
[43] T. Sugawara *et al.*, “Structural basis for pore-forming mechanism of staphylococcal α-hemolysin,” *Toxicon*, vol. 108, pp. 226–231, Dec. 2015, doi: 10.1016/j.toxicon.2015.09.033.
[44] C. Meesters, A. Brack, N. Hellmann, and H. Decker, “Structural characterization of the α-hemolysin monomer from Staphylococcus aureus,” *Proteins Struct. Funct. Bioinforma.*, vol. 75, no. 1, pp. 118–126, 2009, doi: 10.1002/prot.22227.

[45] L. Song, M. R. Hobaugh, C. Shustak, S. Cheley, H. Bayley, and J. E. Gouaux, “Structure of Staphylococcal α-Hemolysin, a Heptameric Transmembrane Pore,” *Science*, vol. 274, no. 5294, pp. 1859–1865, Dec. 1996, doi: 10.1126/science.274.5294.1859.
[46] G. A. Wilke and J. B. Wardenburg, “Role of a disintegrin and metalloprotease 10 in Staphylococcus aureus α-hemolysin–mediated cellular injury,” *Proc. Natl. Acad. Sci.*, vol. 107, no. 30, pp. 13473–13478, Jul. 2010, doi: 10.1073/pnas.1001815107.
[47] Y.-C. Chiu *et al.*, “Structural basis for calcium-stimulating pore formation of Vibrio α-hemolysin,” *Nat. Commun.*, vol. 14, no. 1, p. 5946, Sep. 2023, doi: 10.1038/s41467-023-41579-x.
[48] F. Essmann *et al.*, “Staphylococcus aureus α-toxin-induced cell death: predominant necrosis despite apoptotic caspase activation,” *Cell Death Differ.*, vol. 10, no. 11, pp. 1260–1272, Nov. 2003, doi: 10.1038/sj.cdd.4401301.
[49] “Alpha Hemolysin.” Accessed: May 17, 2026. [Online]. Available: https://www.cmu.edu/biolphys/smsl/research/topics/hemolysin.html
[50] D. J. McGillivray *et al.*, “Structure of Functional Staphylococcus aureus α-Hemolysin Channels in Tethered Bilayer Lipid Membranes,” *Biophys. J.*, vol. 96, no. 4, pp. 1547–1553, Feb. 2009, doi: 10.1016/j.bpj.2008.11.020.
[51] A. Chatterjee *et al.*, “Structural insights into pre-pore intermediates of alpha-hemolysin in the lipidic environment,” *Nat. Commun.*, vol. 16, no. 1, p. 6348, Jul. 2025, doi: 10.1038/s41467-025-61741-x.
[52] G. van den Bogaart, J. V. Guzmán, J. T. Mika, and B. Poolman, “On the Mechanism of Pore Formation by Melittin *”, Accessed: May 17, 2026. [Online]. Available: https://www.jbc.org/article/S0021-9258(20)65238-3/abstract
[53] K. Sugihara, M. Delai, I. Szendro, O. Guillaume-Gentil, J. Vörös, and T. Zambelli, “Simultaneous OWLS and EIS monitoring of supported lipid bilayers with the pore forming peptide melittin,” *Sens. Actuators B Chem.*, vol. 161, no. 1, pp. 600–606, Jan. 2012, doi: 10.1016/j.snb.2011.11.007.
[54] Z. Zhu, Z. Hu, S. Li, R. Fang, H. K. Ono, and D.-L. Hu, “Molecular Characteristics and Pathogenicity of Staphylococcus aureus Exotoxins,” *Int. J. Mol. Sci.*, vol. 25, no. 1, p. 395, Dec. 2023, doi: 10.3390/ijms25010395.
[55] A. Magni *et al.*, “A membrane intercalating metal-free conjugated organic photosensitizer for bacterial photodynamic inactivation,” *Chem. Sci.*, vol. 14, no. 30, pp. 8196–8205, doi: 10.1039/d3sc01168b.
[56] P. Me *et al.*, “Nanoactuator for Neuronal Optoporation,” *PubMed*, 2024, Accessed: May 18, 2026. [Online]. Available: https://pubmed.ncbi.nlm.nih.gov/38687909/
[57] R. N. Moman, N. Gupta, C. Singh, and M. A. Varacallo, “Physiology, Albumin,” in *StatPearls*, Treasure Island (FL): StatPearls Publishing, 2026. Accessed: May 17, 2026. [Online]. Available: http://www.ncbi.nlm.nih.gov/books/NBK459198/
[58] S. Curry, H. Mandelkow, P. Brick, and N. Franks, “Crystal structure of human serum albumin complexed with fatty acid reveals an asymmetric distribution of binding sites,” *Nat. Struct. Biol.*, vol. 5, no. 9, pp. 827–835, Sep. 1998, doi: 10.1038/1869.
[59] F. Bonté and R. L. Juliano, “Interactions of liposomes with serum proteins,” *Chem. Phys. Lipids*, vol. 40, no. 2, pp. 359–372, Jun. 1986, doi: 10.1016/0009-3084(86)90079-4.
[60] S. A. Onaizi, M. S. Nasser, and F. Twaiq, “Lysozyme binding to tethered bilayer lipid membranes prepared by rapid solvent exchange and vesicle fusion methods,” *Eur. Biophys. J.*, vol. 43, no. 4, pp. 191–198, Mar. 2014, doi: 10.1007/s00249-014-0955-z.
[61] I. K. Vockenroth, D. Fine, A. Dodobalapur, A. T. A. Jenkins, and I. Köper, “Tethered bilayer lipid membranes with giga-ohm resistances,” *Electrochem. Commun.*, vol. 10, no. 2, pp. 323–328, Feb. 2008, doi: 10.1016/j.elecom.2007.12.018.

[62] A. Aleksandrovic, I. Gabriunaite, G. Valincius, and A. Valiūnienė, “Regeneration of tethered bilayer lipid membrane biosensors for repetitive use in toxin detection,” *Bioelectrochemistry*, vol. 167, p. 109078, Feb. 2026, doi: 10.1016/j.bioelechem.2025.109078.
[63] J. Drelich, J. L. Wilbur, J. D. Miller, and G. M. Whitesides, “Contact Angles for Liquid Drops at a Model Heterogeneous Surface Consisting of Alternating and Parallel Hydrophobic/Hydrophilic Strips,” *Langmuir*, vol. 12, no. 7, pp. 1913–1922, Jan. 1996, doi: 10.1021/la9509763.
[64] J. Drelich and E. Chibowski, “Superhydrophilic and Superwetting Surfaces: Definition and Mechanisms of Control,” *Langmuir*, vol. 26, no. 24, pp. 18621–18623, Dec. 2010, doi: 10.1021/la1039893.
[65] S. M. Lößlein, R. Merz, D. W. Müller, M. Kopnarski, and F. Mücklich, “An in-depth evaluation of sample and measurement induced influences on static contact angle measurements,” *Sci. Rep.*, vol. 12, no. 1, p. 19389, Nov. 2022, doi: 10.1038/s41598-022-23341-3.
[66] M. Vuckovac, M. Latikka, K. Liu, T. Huhtamäki, and R. H. A. Ras, “Uncertainties in contact angle goniometry”, doi: 10.1039/C9SM01221D.
[67] F. E. Bartell and J. T. Smith, “Alteration of Surface Properties of Gold and Silver as Indicated by Contact Angle Measurements,” *J. Phys. Chem.*, vol. 57, no. 2, pp. 165–172, Feb. 1953, doi: 10.1021/j150503a008.
[68] L. Zhang, A. G. Zhou, B. R. Sun, K. S. Chen, and H.-Z. Yu, “Functional and versatile superhydrophobic coatings via stoichiometric silanization,” *Nat. Commun.*, vol. 12, no. 1, p. 982, Feb. 2021, doi: 10.1038/s41467-021-21219-y.
[69] B. Wu, G. Mao, and K. Y. S. Ng, “Stepwise adsorption of a long trichlorosilane and a short aminosilane,” *Colloids Surf. Physicochem. Eng. Asp.*, vol. 162, no. 1, pp. 203–213, Mar. 2000, doi: 10.1016/S0927-7757(99)00240-X.
[70] M. E. van der Boom, G. Evmenenko, C. Yu, P. Dutta, and T. J. Marks, “Interrupted-Growth Studies of the Self-Assembly of Intrinsically Acentric Siloxane-Derived Monolayers,” *Langmuir*, vol. 19, no. 25, pp. 10531–10537, Dec. 2003, doi: 10.1021/la034900f.
[71] R. Budvytyte *et al.*, “Structure and Properties of Tethered Bilayer Lipid Membranes with Unsaturated Anchor Molecules,” *Langmuir*, vol. 29, no. 27, pp. 8645–8656, Jul. 2013, doi: 10.1021/la401132c.
[72] I. K. Vockenroth, C. Rossi, M. R. Shah, and I. Köper, “Formation of tethered bilayer lipid membranes probed by various surface sensitive techniques,” *Biointerphases*, vol. 4, no. 2, pp. 19–26, Apr. 2009, doi: 10.1116/1.3122019.
[73] J. Jass, T. Tjärnhage, and G. Puu, “From Liposomes to Supported, Planar Bilayer Structures on Hydrophilic and Hydrophobic Surfaces: An Atomic Force Microscopy Study”, Accessed: May 17, 2026. [Online]. Available: https://www.cell.com/biophysj/abstract/S0006-3495(00)76549-0
[74] M. B. Smith, K. Efimenko, D. A. Fischer, S. E. Lappi, P. K. Kilpatrick, and J. Genzer, “Study of the Packing Density and Molecular Orientation of Bimolecular Self-Assembled Monolayers of Aromatic and Aliphatic Organosilanes on Silica,” *Langmuir*, vol. 23, no. 2, pp. 673–683, Jan. 2007, doi: 10.1021/la062475v.
[75] J. T. Woodward, H. Gwin, and D. K. Schwartz, “Contact Angles on Surfaces with Mesoscopic Chemical Heterogeneity,” *Langmuir*, vol. 16, no. 6, pp. 2957–2961, Mar. 2000, doi: 10.1021/la991068z.
[76] D. McGillivray *et al.*, “Molecular-scale Structural and Functional Characterization of Sparsely Tethered Bilayer Membranes,” *NIST*, Oct. 2021, Accessed: May 17, 2026.

[Online]. Available: https://www.nist.gov/publications/molecular-scale-structural-and-functional-characterization-sparsely-tethered-bilayer-0
[77] Z. Hetzler, N. Lott, A. Dey Poonam, S. Dalgan, and Q. Wei, "Single-use biosensors for biomanufacturing: Perspective on the state-of-the-art," *Curr. Opin. Biomed. Eng.*, vol. 28, p. 100512, Dec. 2023, doi: 10.1016/j.cobme.2023.100512.
[78] Y. Jia, S. Chen, Q. Wang, and J. Li, "Recent progress in biosensor regeneration techniques", doi: 10.1039/D3NR05456J.
[79] A. Aleksandrovic, I. Gabriunaite, G. Valincius, and A. Valiūnienė, "Regeneration of tethered bilayer lipid membrane biosensors for repetitive use in toxin detection," *Bioelectrochemistry*, vol. 167, p. 109078, Feb. 2026, doi: 10.1016/j.bioelechem.2025.109078.
[80] C. Liu, X. Liu, Y. Qin, C. Deng, and J. Xiang, "A simple regenerable electrochemical aptasensor for the parallel and continuous detection of biomarkers", doi: 10.1039/C6RA09284E.
[81] J. Andersson, I. Köper, and W. Knoll, "Frontiers | Tethered Membrane Architectures—Design and Applications", doi: 10.3389/fmats.2018.00055.
[82] A. P. Shivabalan, F. Ambrulevičius, M. Talaikis, V. Pudžaitis, G. Niaura, and G. Valinčius, "Effect of pH on electrochemical impedance response of tethered bilayer lipid membranes: implications for quantitative biosensing", Accessed: May 17, 2026. [Online]. Available: https://epublications.vu.lt/object/elaba:180095319/index.html
[83] I. Gabriunaite *et al.*, "Sensitivity of lipid bilayer sensing of pore-forming toxins relies on electrical properties of nanoscale-thick submembrane reservoir separating solid support and phospholipid membrane," *Electrochimica Acta*, vol. 526, p. 146189, Jun. 2025, doi: 10.1016/j.electacta.2025.146189.
[84] V. G, M. T, and I. F, "Electrochemical impedance spectroscopy of tethered bilayer membranes," *PubMed*, 2012, Accessed: May 17, 2026. [Online]. Available: https://pubmed.ncbi.nlm.nih.gov/22126190/
[85] D. A. Dickie, A. Y. C. Chan, H. Jalali, H. A. Jenkins, H.-Z. Yu, and J. A. C. Clyburne, "m-Terphenyl thiols: rigid and bulky molecules for the formation of bioactive self-assembled monolayers on gold", doi: 10.1039/B410264A.
[86] C. Vericat *et al.*, "Self-assembled monolayers of thiolates on metals: a review article on sulfur-metal chemistry and surface structures", doi: 10.1039/C4RA04659E.
[87] M. S. Inkpen, Z.-F. Liu, H. Li, L. M. Campos, J. B. Neaton, and L. Venkataraman, "Non-chemisorbed gold–sulfur binding prevails in self-assembled monolayers," *Nat. Chem.*, vol. 11, no. 4, pp. 351–358, Apr. 2019, doi: 10.1038/s41557-019-0216-y.
[88] "Molecular Anchors for Self-Assembled Monolayers on ZnO: A Direct Comparison of the Thiol and Phosphonic Acid Moieties | The Journal of Physical Chemistry C." Accessed: May 18, 2026. [Online]. Available: https://pubs.acs.org/doi/10.1021/jp906013r
[89] A. Chandekar, S. K. Sengupta, and J. E. Whitten, "Thermal stability of thiol and silane monolayers: A comparative study," *Appl. Surf. Sci.*, vol. 256, no. 9, pp. 2742–2749, Feb. 2010, doi: 10.1016/j.apsusc.2009.11.020.
[90] J. A. Jackman, W. Knoll, and N.-J. Cho, "Biotechnology Applications of Tethered Lipid Bilayer Membranes," *Materials*, vol. 5, no. 12, pp. 2637–2657, Dec. 2012, doi: 10.3390/ma5122637.
[91] S. Saem, O. Shahid, A. Khondker, C. Moran-Hidalgo, M. C. Rheinstädter, and J. Moran-Mirabal, "Benchtop-fabricated lipid-based electrochemical sensing platform for the detection of membrane disrupting agents," *Sci. Rep.*, vol. 10, no. 1, p. 4595, Mar. 2020, doi: 10.1038/s41598-020-61561-7.

[92] S. Jafari *et al.*, “ASSURED Point-of-Need Food Safety Screening: A Critical Assessment of Portable Food Analyzers,” *Foods*, vol. 10, no. 6, p. 1399, Jun. 2021, doi: 10.3390/foods10061399.
[93] “*Staphylococcus aureus* alpha toxin,” *Wikipedia*. Apr. 25, 2025. Accessed: May 18, 2026. [Online]. Available: https://en.wikipedia.org/w/index.php?title=Staphylococcus_aureus_alpha_toxin&oldid=1287275030
[94] G. Ziziunaite, G. Valincius, and A. Valiūnienė, “Predictive physical parameters for reproducible electrochemical detection of α-hemolysin with tBLMs on FTO substrates,” *Electrochimica Acta*, vol. 549, p. 148019, Feb. 2026, doi: 10.1016/j.electacta.2025.148019.
[95] A. Ulman, “Formation and Structure of Self-Assembled Monolayers,” *Chem. Rev.*, vol. 96, no. 4, pp. 1533–1554, Jan. 1996, doi: 10.1021/cr9502357.
[96] I. K. Vockenroth, P. P. Atanasova, A. T. A. Jenkins, and I. Köper, “Incorporation of α-Hemolysin in Different Tethered Bilayer Lipid Membrane Architectures,” *Langmuir*, vol. 24, no. 2, pp. 496–502, Jan. 2008, doi: 10.1021/la7030279.
[97] “A biosensor that uses ion-channel switches | Nature.” Accessed: May 18, 2026. [Online]. Available: https://www.nature.com/articles/42432
[98] M. E. Pfeffer *et al.*, “Nanoactuator for Neuronal Optoporation,” *ACS Nano*, vol. 18, no. 19, pp. 12427–12452, May 2024, doi: 10.1021/acsnano.4c01672.